NTNU
Det skapende universitet

# Comparison of the stress distribution in the metallic layers of flexible pipes using two alternative Bflex formulations

Yunzhu Shi

Marine Technology
Innlevert: juni 2014
Hovedveileder: Svein Sævik, IMT

Norges teknisk-naturvitenskapelige universitet
Institutt for marin teknikk

NTNU
Norwegian University of
Science and Technology

# Comparison Of The Stress Distribution In The Metallic Layers Of Flexible Pipes Using Two Alternative Bflex Formulations

Yunzhu Shi

June 2014

MASTER THESIS

Department of Marine Technology

Norwegian University of Science and Technology

Supervisor 1: Professor Svein Sævik

Supervisor 2: Professor Naiquan Ye

# MASTER THESIS SPRING 2014

**for**

**Stud. tech. Yunzhu Shi**

**Comparison of the stress distribution in the metallic layers of flexible pipes using two alternative Bflex formulations**

*Sammenligningavspenningsfordelingengjennomtverrsnittetmedbrukavtre alternativeBflexformuleringer*

The strength of flexible pipes is primarily governed by the axial stresses of the metallic layers. In Bflex there are two principally different models for calculating the stresses in a flexible pipe:

1. Establishing a model for the core and tensile armour layers (FLEXCROSS, ITCODES 21,31,0 and1). This model is used to calculate both axisymmetric (pressure, tension and torsion) stresses and stresses due to bending and friction in the tensile armours. The contact pressures and the stresses in other layers due to axisymmetric loads are established by a 2D layered model.
2. Establish a simplified model for all layers of the flexible (353FLEXCROSS, no itcode)

This project work is to be carried out as follows:

1. Literature study into flexible pipe mechanical response, associated design criteria and analytical as well as computational techniques for calculating the stresses in the metallic layers. Methods for calculating both axisymmetric and bending stresses from literature as well as the ones formulated in Bflex is to be included in the study.
2. Establish necessary input for flexible riser local stress analysis. Different pipe cross-sections is to be evaluated covering different relevant dimensions/applications. The cross-sections shall be the same as the ones used by Liu Xiaoli and Lidong Wang Therefore the three of you should cooperate using the same cross-section input. A full and detailed overview of the cross-section input and load cases analysis shall be included in the report.
3. Establish local Bflex models for the flexible pipe cross-section using (FLEXCROSS, ITCODES 31 and 0) and the new full FE (353FLEXCROSS eltypes HSHEAR353, H-CONT463 and HSHEAR463 no ITCODE) assumptions.
4. Define stub models in Bflex for the above cross-sections and perform stress analysis

for internal pressure, external pressure and tension load cases and compare the results in terms of axial stress history plots showing the results from the different models in the same plot. Results from all metallic layers is to be included (use Bpost). Also include the results from analytical calculations in the same plot.
5. Conclusions and recommendations for further work

The work scope may prove to be larger than initially anticipated. Subject to approval from the supervisors, topics may be deleted from the list above or reduced in extent.

In the thesis the candidate shall present his personal contribution to the resolution of problems within the scope of the thesis work

Theories and conclusions should be based on mathematical derivations and/or logic reasoning identifying the various steps in the deduction.

The candidate should utilise the existing possibilities for obtaining relevant literature.

Thesis format
The thesis should be organised in a rational manner to give a clear exposition of results, assessments, and conclusions. The text should be brief and to the point, with a clear language. Telegraphic language should be avoided.

The thesis shall contain the following elements: A text defining the scope, preface, list of contents, summary, main body of thesis, conclusions with recommendations for further work, list of symbols and acronyms, references and (optional) appendices. All figures, tables and equations shall be numerated.

All plots shall be separately stored electronically in jpg format using self explaining filenames. It is also preferred that the thesis is written in Latex (not mandatory) and all files are to be delivered together with the report.

The supervisors may require that the candidate, in an early stage of the work, presents a written plan for the completion of the work.

The original contribution of the candidate and material taken from other sources shall be clearly defined. Work from other sources shall be properly referenced using an acknowledged referencing system.

The report shall be submitted in two copies: - Signed by the candidate - The text defining the scope included - In bound volume(s) - Drawings and/or computer prints which cannot be bound should be organised in a separate folder.

Ownership
NTNU has according to the present rules the ownership of the thesis. Any use of the thesis has to be approved by NTNU (or external partner when this applies). The department has the right to use the thesis as if the work was carried out by a NTNU employee, if nothing else has been agreed in advance.

Thesis supervisors
Prof. Svein Svik, NTNU.
Dr. Naiquan Ye, Marintek

Deadline: June 10th, 2014

Trondheim, January, 2014

Svein Sævik

## Acknowledgement

The thesis was written in spring 2014. The scope was proposed by my supervisor Svein Sævik at Norwegian University of Science and Technology (NTNU), Department of Marine Technology. The assignment was to investigate the stress distribution in all metallic layers of flexible pipe. The initial months of work were spend on literature study into mechanical properties of flexible pipe and finite element modelling method of flexible pipe. The rest of work consisted of modelling and result analysis.

Sincere thanks to my supervisor Svein Sævik. His patient explanation and valuable suggestion are acknowledged.

Sincere thanks are also given to my second supervisor Naiquan Ye. His assistance and arrangement help me deliver the thesis on time

I am also very grateful to my classmates for valuable discussion.

## Abstract

Axisymmetric load is the most common load acting on flexible pipe. Modelling axisymmetric load correctly is very important to estimate the strength of a flexible pipe. The purpose of the thesis is to compare the stress distribution in metallic layers under three load case, i.e. tension, internal pressure and external pressure. Literature study and discussion to mechanical properties of flexible pipe and finite element modelling method are included in the thesis. The modelling program is BFLEX program. Models for three flexible pipes are built in BFLEX for 6inch pipe, 8inch pipe and 16inch pipe. Different element models are applied to model metallic layers. Element PIPE52 are used to model all metallic layers for ITCODE31 model. For ITCODE0 model, element PIPE52 are used to model carcass and pressure armour; element HSHEAR352 is used to model helical tensile layer. For full FE model, carcass and pressure armour are modelled by element HSHEAR363 and tensile layer is modelled by element HSHEAR353. For ITCODE31 and ITCODE0 models, the computing stress is taken from local model after BPOST. For full FE model, the stress is from global model directly. Moreover, analytical solution is found to estimate the modelling performance.

# Contents

# List of Figures

# List of Tables

# Chapter 1

# Introduction

## 1.1 Flexible Pipe Technology

Offshore pipelines are used for oil and gas transport worldwide. Depending on application, pipelines can be classified into[1]:

- Export pipelines: large diameter lines exporting processed oil and gas from the offshore installation to the onshore processing plant to the market.
- Flowlines: small diameter lines transporting the unprocessed well flow from the wellhead to the offshore processing plant.
- Intra-field line: for transport between offshore installations.
- Chemical injection lines: providing anti-freeze and corrosion inhibitors that are injected into the pipeline/flowline wellstream to control hydrate (ice) formation and corrosion
- Water injection lines: for pumping water into the reservoir to keep the reservoir pressure and improve the production rate.
- Bundles: normally based on installing the flowline, umbilical and injection lines into one pipe cross-section, a carrier pipe that provides mechanical protection and installation buoyancy.

Illustration of application of flexible pipe in offshore industry:

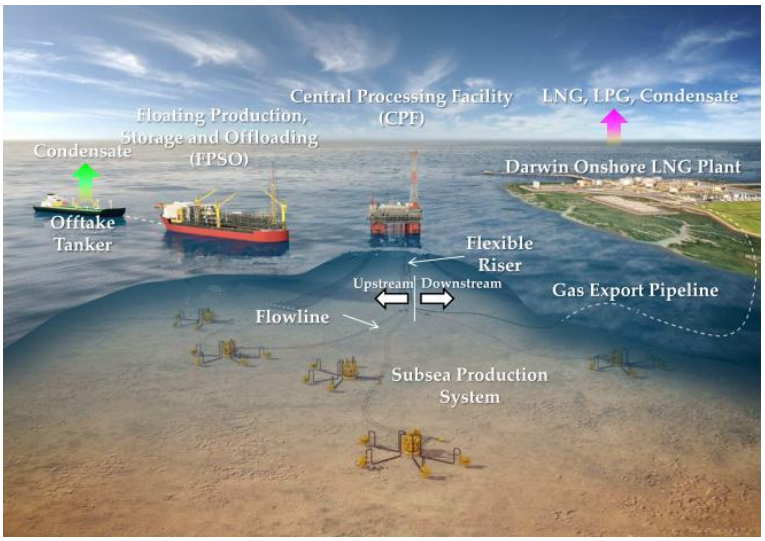


**Figure 1.1:** Different types of flexible pipes

Flexible pipes are widely applied in well around the world because of their advantages compared to traditional rigid pipes. Flexible pipes are more corrosion resistant and have superior flow characteristics. One big advantage of flexible pipes over rigid pipes is installation. the installation process is rapid because of the flexibility, usually 5 to 10 km per day. And their ease of installation and elimination of field welds results in great economy.

The durable polymer sheath outsides the steel protect the steel from cathodic corrosion. In this way, the cathodic protection and most coating repairs are eliminated. Additionally, flexible pipes have superior flow characteristics because of the smooth inner liner, which has low friction and is augmented by the thermal insulating properties of the pipe retaining heat and minimizing viscosity of conveyed hydrocarbons. And because of the inner and outer sheaths, which offer flexible pipes good corrosion resistance, flexible pipes have a longer life and higher reliability than rigid pipes. Moreover, the total cost of the installation of flexible pipes is half rigid pipes. the installation saving is largely from storing and handling long lengths of pipe on a reel and minimizing the number of field joints with the attendant labor requirement. Besides, because of the good corrosion resistance, the cost of operating is reduced, and the cost of periodic inspection and maintenance is reduced to minimum. Traditional flexible pipes have been applied in tough offshore environment for decades and often used as dynamic risers to tie the fixed subsea facilities to floating facilities. Therefore, flexible pipes have many offshore experience with many applications which have been practiced over decades.

Overall, we can see that flexible pipes of big advantages over rigid pipes both on economy and flow characteristics. With the advantages, more and more flexible pipes are installed around the world. The point to study the stress distribution of metallic layers is to investigate how the metallic layers behave when subjected external load during installation or operation, giving references to pipe installation and design.

## 1.2 The Scope of Work

The study of the thesis is aiming to investigate the axial stress distribution in metallic layers of flexible pipes. Briefly, the work has been done includes building models for three flexible pipes (6inch, 8inch and 16inch) in BFLEX program, computing the axial stress under three load cases which are tension-only, internal pressure-only and external pressure-only respectively and calculating the analytical solution for each load case. In building model part, 6 types of element are used to model metallic layers (carcass, pressure armour and tensile layer) and parameters of three cross-section (thickness, number of tendon, lay angle, etc) are defined in BFLEX program (FLEXCROSS for ITCODE31 and ITCODE0, 353FLEXCROSS for full FE). In computing part, three load cases are defined, including a pipe subjected tension only, internal pressure only and external pressure only. MATLAB program is used to extract the data from the mpf files which are generated by BFLEX program containing the values of computing stress and plot the stress as the function of the introduced load (tension, internal pressure and external pressure respectively). In analytical solution calculating part, every analytical solution corresponding to each pipe for certain load case is found. According to the comparison of the stress distribution and analytical solutions, a discussion about element performance in modeling is given.

In chapter1, general introduction about background of application of flexible pipe and the scope of work for the thesis is given.

In chapter2, mechanical properties of flexible pipe is discussed, including response to axial load, torsion and bending. Additionally, design criteria and typical failure modes are discussed in the chapter as well.

In chapter3, a theory introduction of BFLEX program is represented. On the other hand, elements used to model are discussed in the chapter, such as the element model, the

property of element.

In chapter4, process of how to model each pipe under every load case is explained, including explanation to choose parameters, how to determine the computing time, etc.

In chapter5, analysis of result will be performed. The cause of deviation will be discussed. The comparison with analytical solution is the core of the chapter.

# Chapter 2

# Flexible pipe concept

## 2.1 Cross section properties

A typical cross section of flexible pipe is shown below.

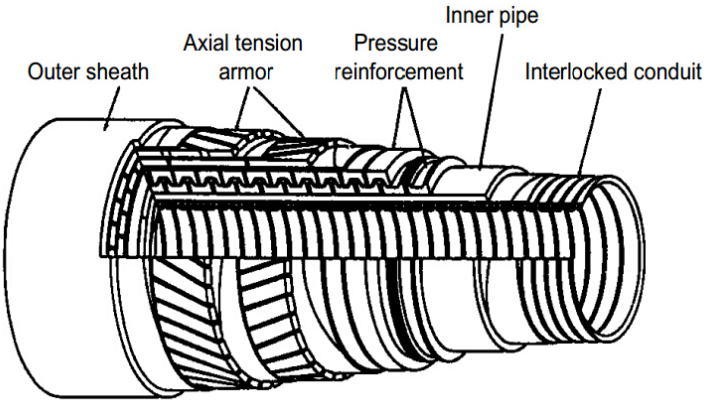


**Figure 2.1:** Typical cross section of a flexible pipe

**1.Carcass**

Interlocked conduit denotes carcass. Carcass is constructed by flat steel trips which are interlocked to prevent the collapse induced by external pressure, installation loads and gas in pipe. The carcass is not leak tight. Therefore, it does not sustain the internal pressure. Based on the assumption of that annulus between outer sheath and pressure bore is water filled, the carcass sustains the whole water pressure alone. Depending on the magnitude of gap between the carcass and other layers, other layers may sustain the

carcass as supports.

**2.Pressure barrier**

The second annulus is pressure barrier, which a sheath annulus. This layer is leak tight.

**3.Pressure armour**

The next annulus is pressure reinforcement which is also called pressure armour. The pressure armour encircle the pressure barrier with 1-2 wires and lay angle is close to 90°. This layer supports the carcass layer when the carcass sustaining the external pressure. Also, it supports the pressure barrier to resist the internal pressure.

**4.Tensile armour**

The fourth layer is tensile armour, which is constructed by two cross-wound layers. The two cross-wound layers maintain balance of torsion. These layers provide the strength for torque, tension and pressure end cap force. Generally, there are 30-80 steel wires in each layer. And the lay angle ranges from ±20° to ±60° (positive sign follows the right hand rule).

**5.External sheath**

The outer layer is external sheath. This layer is to prevent the inside metallic layers from corrosion and abrasion.

## 2.2 Mechanical properties of flexible pipes

### 2.2.1 Axial loads

According to the study of Sævik [2], when a flexible pipe is subjected to a tension, the helical tensile armour is the layer that mainly carry the tension load. The plastic layers provide a very small part of resistance which is negligible. The stress in the tensile layer created by the tension is in radial direction which is analogous to external pressure. Under this case of mechanism, there are two modes for pipe failure:

1. Rapture of tensile armours due to the exceeding of the ultimate breaking strength.

2. Buckling of the pipe due to that the stress created by the tension exceeds the buckling strength of the pipe.

However, in normal case, the two failure modes are not critical problem for flexible pipes since the pipes are normally built in large radial load capacity.In tension-only case, the axial resistance from all $N_a$ resisting layers must equal to the true pipe wall force $T_w$.

$$\sum n_i \sigma_i A_i \cos \alpha_i = T_w = T_e + \pi P_{int} r_{int}^2 - \pi P_{ext} r_{ext}^2 \tag{2.2.1}$$

where

- $n_i$=number of tendons in layer i
- $\sigma_i$=tensile stress in tendon
- $A_i$=cross section area of a tendon
- $\alpha_i$=lay angle
- $T_e$=effective tension
- $P_{int}, P_{ext}$=internal/external pressure
- $r_{int}, r_{ext}$=internal/external pressure radius

Figure below shows a pipe subjected to an axial force $T_e$ (effective tension).

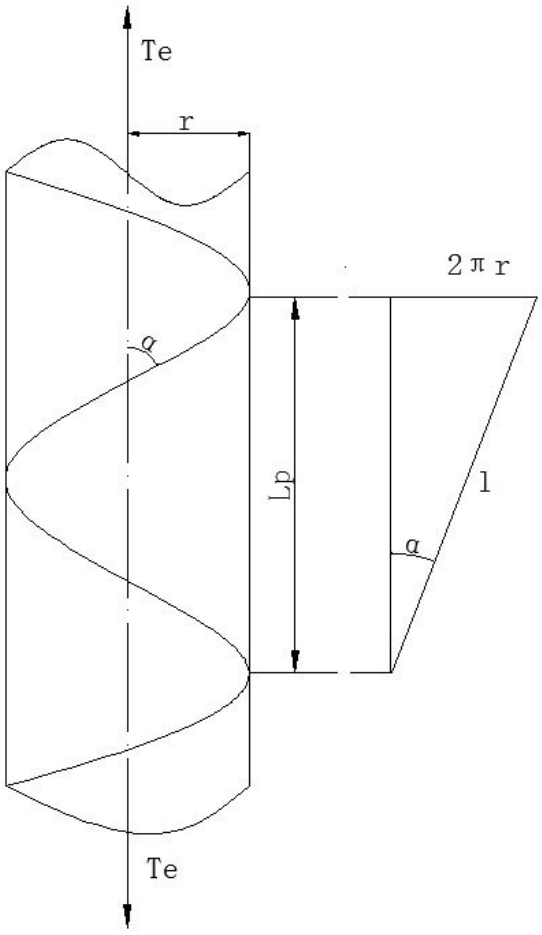


**Figure 2.2:** Effective tension

Normally, the lay angle for pressure armours are wound at $\alpha = 90°$, which could not make too much contribution to radial load capacity. For a non-bonded pipe, the following formulation can be used to evaluate the stress in the tensile layers:

$$\sigma_t = \frac{T_w}{nA_t \cos\alpha} \tag{2.2.2}$$

or

$$\sigma_t = \frac{T_w}{2tF_f \pi r \cos^2\alpha} \tag{2.2.3}$$

where n is the total number of tendons in the armouring layers, $A_t$ is the cross section area of the tendon, t is the total thickness of the tensile armours. the value of $F_f$ gives the fraction of surface area covered by tendons so that it takes into account the non-

contributing gaps between neighbouring tendons. the value of factor is normally taken 0.9 for a non-bonded pipe. when a flexible pipe is subjected to a tension, the lay angle of the tensile armour tends to decrease. however, due to the underlying layers, which are the carcass and pressure layers, the decrease of the lay angle can be prevented. On the pressure layers and carcass, the the external pressure created by the tension can be evaluated approximately by the formulation:

$$P_T = \frac{T_w t g^2 \alpha}{2\pi r^2} \tag{2.2.4}$$

For non-bonded pipes, the resistance to the external pressure $p_T$ is shared between the pressure layers and the carcass.

An estimate of axial stiffness can be found by use of Eq.(2.2.2). The following expression links the tendon stresses and the pipe deformation.

$$\frac{\sigma}{E} = \cos^2\alpha \frac{\Delta L}{L} + \sin^2\alpha + r\sin\alpha\cos\alpha\frac{\Delta\theta}{L} \tag{2.2.5}$$

$\Delta L$, $\Delta r$, and $\Delta\theta$ are the global axial, radial and torsional pipe deformations. the following expression is for the axial stiffness neglecting the torsional deformation $\Delta\theta$:

$$EA = nEA_t\cos\alpha(\cos^2\alpha - v\sin^2\alpha) \tag{2.2.6}$$

where the apparent Poisson ratio is defined as:

$$v = -\frac{\frac{\Delta r}{r}}{\frac{\Delta L}{L}} \tag{2.2.7}$$

In Eq.(1.2.6), the first term responds to the elongation of the tensile wires and the second term responds to the increase in axial length associated with a decrease in tensile layer diameter. The value of $v$ depends on the response of the underlying layers to the squeezing pressure from the tensile wires. For non-bonded pipes which is subjected to radial pressure, the value of $v$ is taken as small ($\approx$0.2). Consequently, the first term will dominate. However, it should be noted that Eq.(2.2.6) is under the assumption of small

geometric deformations.

### 2.2.2 Internal pressure

When a pipe is subjected to internal pressure, the load will carried by the tensile armours and the pressure armours. the failure mode which is associated with the internal pressure is bursting. When the maximum pressure is considerably underestimated, bursting is likely to occur. According to API, the bursting pressure should be at least 2 times the design pressure. Therefore, if the internal pressure is known, bursting can be avoided. It is noted that the design pressure should include operating pressure and other factors which may affect internal pressure. Additionally, the design pressure should be combined with atmospheric external pressure. the equilibrium between stresses and the radial forces is given as:

$$\sum_{i=1}^{N_r} \frac{n_i \sigma_i A_i \sin\alpha_i \tan\alpha_i}{2\pi r_i} = P_{int} r_{int} - P_{ext} r_{ext} \tag{2.2.8}$$

Where $N_r$ is the number of pressure resisting layers. Plastic sheaths only transmit pressure is assumed for approximation, consequently, the carcass does not carry any internal pressure. Therefore, for non-bonded flexible pipes, the pressure layers and the tensile armour layers must carry internal pressure.

The following expression can be used to determine the number of tendon in a helical armour:

$$n_i = \frac{2\pi r_i}{W_i} F_f \cos\alpha_i \tag{2.2.9}$$

where $W_i$ is the width of each tendon. the contribution of helical armour to burst pressure resistance can be obtained by combing Eq.(1.2.8)and (1.2.9).

$$P_h = \frac{t}{r} F_f \sigma_u \sin^2\alpha \tag{2.2.10}$$

Where t is the total thickness of the helical armour, r is the mean radius of the helical

armour layers and $\Sigma_u$ is the ultimate tensile strength of the layer. For the contribution of the helical armour to endcap pressure resistance, Eq.(2.2.3) can be used:

$$P_a = 2\frac{r}{r_{int}^2} t F_f \sigma_u \cos\alpha^2 \tag{2.2.11}$$

If there are no zeta or back-up pressure layer, the stress in the helical armours must balance the hoop and endcap effects of the internal pressure alone. That is $p_h = p_a$. It gives $\tan\alpha^2 = 2$ by assuming $r_{int} \approx r$, that is $\alpha = 54.7°$. This is the "neutral" or "balanced" lay angle under the situation that there is no tendency for the helical armour to change shape under load. However, the balanced lay angle depends on the amount of steel in the helical armour layers and the pressure layers since a pipe is normally reinforced by several layers.

The contribution to burst pressure resistance from the zeta layer or the back-up pressure layer, $P_z$ or $P_u$, can be obtained by the following expression:

$$P_z = \frac{t}{r} F_f \sigma_u \tag{2.2.12}$$

Where t and r denote the thickness and the mean radius of the pressure layer respectively. The total hoop pressure resistance is then obtained by summing the contribution from each layer.

$$P_{hoop} = P_z + P_{bu} + P_h \tag{2.2.13}$$

The burst pressure is given by the smaller of $P_{hoop}$ and $P_a$, i.e. hoop and axial resistance

$$P_b = min(P_{hoop}, P_a) \tag{2.2.14}$$

In pipe design, the lay angle is normally chosen to give equal burst resistance in the axial and hoop directions. The calculation for burst pressure above is simple and approximated. However, experimental results showed that the calculations gives reliable estimates.

### 2.2.3 External pressure

When a pipe is subjected to external pressure, the load are normally carried by the interlocked carcass and pressure layers, which both have a lay angle close to 90°. Considered the situation that the outer sheaths may have been damaged in such way that the external pressure acts on the inner plastic layer directly, the collapse pressure is taken as the collapse strength of the interlocked carcass without counting the contribution from the zeta layer and the back-up pressure layer. Therefore, the interlocked carcass is normally designed to carry the full external pressure alone.

Large external pressure may cause collapse of the pipe. Once the pipe collapsed, the flow inside the pipe could not go through the pipe. However, this is not a critical failure mode since the external pressure could be calculated by the design depth. According to API, the safety factor for external pressure is taken to be at least 1.5, which is smaller than the value for bursting strength.

By assuming that there is no restraining effect from the outer layers, the following expression can be used to determined the elastic buckling strength:

$$P_{cr} = \frac{3(EI)_{eq}}{r^3} \tag{2.2.15}$$

Where r is the mean radius of the carcass and $(EI)_{eq}$ is the equivalent ring bending stiffness per unit length of pipe. For a cylinder:

$$(EI)_{eq} = \frac{Et^3}{12(1-v^2)} \tag{2.2.16}$$

Where v is the Poisson ratio.

For the interlocked carcass and the pressure layers:

$$(EI)_{eq} = K \cdot n\frac{EI_n}{L_p} \tag{2.2.17}$$

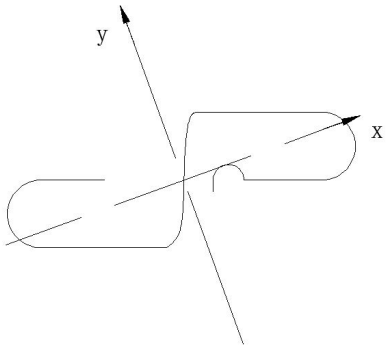


**Figure 2.3:** Interlocked steel profile

Where n is the number of tendons for the layer, $L_p$ is the pitch length and $I_n$ is the smaller moment of inertia of the section, as illustrated in Fig.(2.3) for an interlocked steel profile.

Where K is a factor which depends on the lay angle and the moment of inertia in the section. For massive sections K is close to 1.

The static ring test carried out on a carcass piece can be used to determine the equivalent stiffness. The test consists of measuring the deformation $\delta$ of an interlocked carcass subjected to a radial force F as shown in Fig.(2.4). From the following expression the equivalent ring bending stiffness may be determined:

$$\frac{(EI)_{eq}}{r^3} = (\frac{\pi}{4} - \frac{2}{\pi})\frac{F}{\delta} \tag{2.2.18}$$

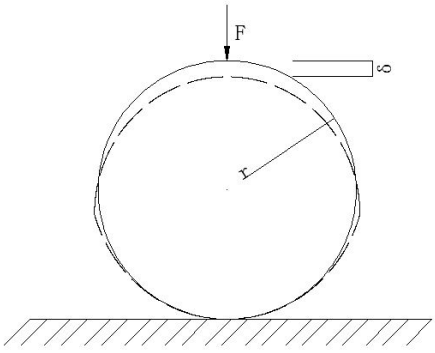


**Figure 2.4:** Static ring test

The give Eq.(2.2.15) overestimates the capacity of the carcass. The true or characteristic buckling strength $P_k$, may be found by a modification of the elastic strength, accounting for inelastic material behaviour and initial ellipticity of the carcass. The following equation suggested by Timoshenko (1950), can be used to determine $P_k$

$$P_k^2 + B \cdot P_k + C = 0 \tag{2.2.19}$$

Where:

$$B = -[\frac{\sigma_y F_f}{m} + (1 + 6mn)P_{cr}] \tag{2.2.20}$$

$$C = \frac{\sigma_f F_f P_{cr}}{m} \tag{2.2.21}$$

$$m = \frac{r}{t} \tag{2.2.22}$$

$$n = \frac{u_0}{r} \tag{2.2.23}$$

$u_0$ is the initial ellipticity, and $\sigma_y$ is the yield strength of the material. This procedure has been adopted by Wellstream, and according to Nielsen et al. (1990), an assumed initial ellipticity $u_0/r = 0.008$ gives a prdicted collapse pressure thar agrees well with experimental results.

The following approach is as an alternative which may assume the pipe to be undamage in such way that the external pressure load acts outside the zeta and back-up pressure layer. Two failure modes are associated with the case:

- 1.Reaching the buckling pressure of the whole pipe
- 2.Reaching the yield stress of the inner layer

For mode 1:

$$P_{cr,p} = \sum_{i=1}^{N_r} P_{cr,i} = \sum_{i=1}^{N_r} \frac{3(EI)_{eq,i}}{r_i^3} \tag{2.2.24}$$

For mode 2:

$$\sigma_t(P_{cr,p}) = -\sigma_y \tag{2.2.25}$$

The smaller one of these two values will be the ultimate pressure. It is noted that only layers having a lay angle close to 90° should be included in Eq.(2.2.24). Another alternative to Eq.(2.2.24) is to carry out a static ring test for the whole pipe, and determine the equivalent stiffness using Eq.(2.2.18). The failure mode for Eq.(2.2.25) assumes the inner layer to be restrained by the outer layers. It is noted that Eq.(2.2.24) gives the elastic pressure resistance. The true pressure strength can be found by using a similar procedure as Eq.(2.2.19).

Finally, as mentioned above, the load created by a tension is analogous to external pressure. Therefore, the total external pressure effect to be used in the capacity check should include the pressure induced by tension and external hydrostatic pressure.

### 2.2.4 Torsion

Excessive torsion may make the tendons lock each other causing "birdcaging" or structural damage to the pipe. However, this is not likely to happen under the normal operational conditions because the torsion loads are small during normal operation. Nevertheless, there have been failure case of a pipe due to the excessive torsion during pipe installation. Current design guidelines specify a torsional strength at least 2 times the design torsional load. An axial tensile force will prevent the pipe from torsional damage. This positive effect is normally taken into account by verifying that the torsional strength for a tensile force smaller than the minimum axial force predicted from the dynamic analysis of the riser system.

Equilibrium between the torsional resistance from all $N_a$ resisting layers and the torsional moment $M_t$:

$$\sum_{i=1}^{N_a} r_i n_i \sigma_i A_i \sin\alpha_i = M_t \tag{2.2.26}$$

The helical wound tensile armours are the main layers to carry the torsional loads. The following expression can be used to make a quick evaluation for the stresses in the tensile

layers:

$$\sigma_t = \frac{M_t}{rnA_t \sin\alpha} \tag{2.2.27}$$

Where n is the total number of tendons in the armouring layers, $A_t$ is the cross section area of each tendon and r is the mean radius of the armouring layers, by combining Eq.(2.2.27) and Eq.(1.2.5), neglecting the $\Delta L/L$ and $\Delta r/r$ terms, the following expression can be used to make an approximate evaluation of the torsional stiffness of the pipe:

$$GI_t = nA_tEr^2 \sin^2\alpha \cos\alpha \tag{2.2.28}$$

It is noted that the formulas above assume that all layers remain in contact. It also should be noted that there is an asymmetry in the torsional stiffness. When a pipe is subjected to a torsion and twist, gaps will occur between the layers. The location of the gaps depends ont he direction of the applied moment.

### 2.2.5 Bending

**Bending behavior of flexible pipes** The bending behavior of flexible pipes is a more complex phenomenon compared to the axisymmetric load case. The flexural response shows a obvious hysteretic behavior, which is illustrated below by the moment/curvature relation.

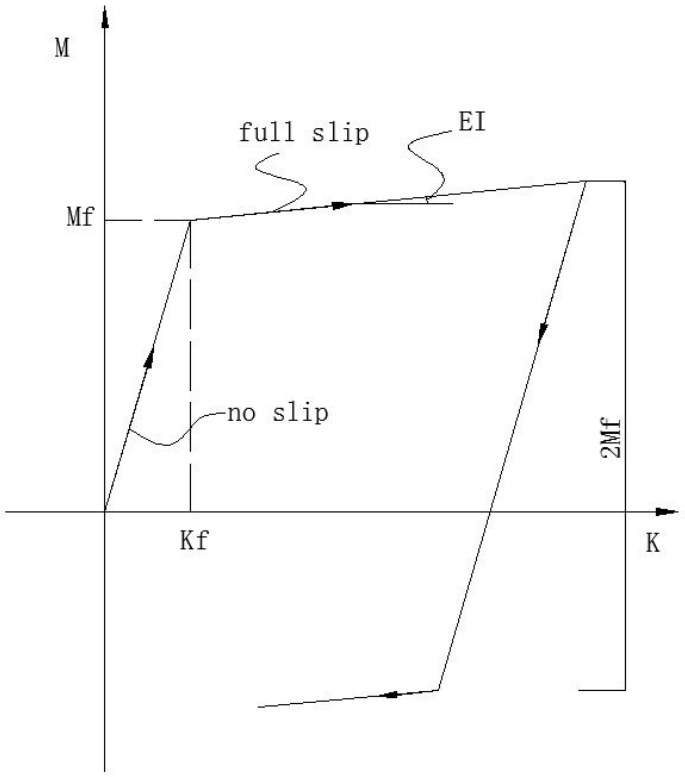


**Figure 2.5:** Hysteretic behavior of flexible pipes

The internal slip mechanism can be used to explain the hysteretic phenomenon of flexible pipes. Such pipes normally have a number of helical reinforcing layers. When the pipe is bent, those layers tend to slip relative to each other. This is particularly the case for the two crosswound tensile layers. At the beginning of bending, the curvatures are small, and the slip is prevented by the internal friction between layers, which reflects a high initial tangent stiffness. The bending moment need to overcome the so-called friction moment $M_f$, which depends on the contact pressure between pipe layers and consequently on the loads applied to the pipe. When the bending moment exceeds the friction moment, the curvature varies linearly with the bending moment. The slope of the hysteretic curve corresponds to the elastic bending stiffness EI. Due to the stiffness of the plastic sheaths, the elastic bending stiffness is rather low. Additionally, when the direction of the curvature is changed, the change in the bending moment has to exceed twice the friction moment before elastic behavior occurs.

**Minimum Bend Radius** Excessive bending may cause local buckling destruction of the pipe as the interlocking elements or helical elements interfere and touch each other.

This is a failure mode which can particularly occur during the handling of the pipe. There are likely large bending near supports and end terminations. Therefore, the bend stiffeners need to be designed properly to keep the bend radius not smaller than the given critical value.

The given critical value is denoted the minimum bend radius $R_{min}$ and is a performance characteristic of the flexible pipe for a given design. The value is specified by the manufacturer aiming to prevent damage under the conditions that the pipe is bent in dynamic, static,installation and storage configurations. Normally, There are several safety factors applied to the minimum bend radius $R_{min}$ for different conditions.

**Minimum Bend Radius for Storage** If the layer geometry is known, the bend radius $R_c$ at which contact occurs between elements within the different helical layers may be calculated. Figure below shows the typical geometries of the interlocked carcass, zeta layer, back-up pressure layer and helical armour layer.

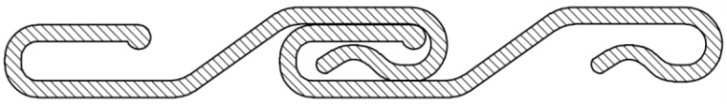

**Figure 2.6:** Typical profile geometries for carcass

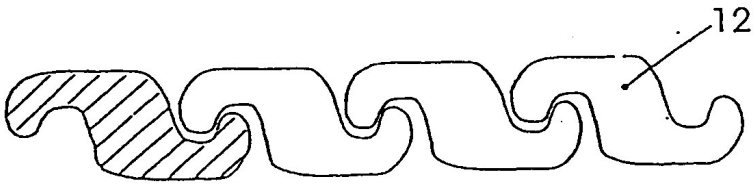


**Figure 2.7:** Typical profile geometries for zeta

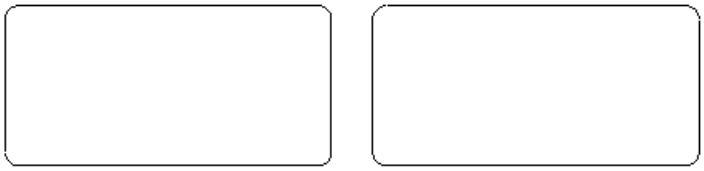

**Figure 2.8:** Typical profile geometries for tensile layer

According to the geometry information, the lateral gap for interlocked profiles can be computed by the following two expressions. The two expressions respectively consider contact on the compression and tensile sides of the pipe.

$$g_{1c} = 1 - \frac{nb_{min}}{2\pi r \cos\alpha} \tag{2.2.29}$$

$$g_{1t} = \frac{nb_{max}}{2\pi r \cos\alpha} - 1 \tag{2.2.30}$$

Where n is the number of tendons in the layer, r is the mean layer radius and $\alpha$ is the lay angle. Then the governing lateral gap is:

$$g_1 = min(g_{1c}, g_{1t}) \tag{2.2.31}$$

For the profiles that are not interlocked the lateral gap becomes:

$$g_1 = 1 - \frac{nb}{2\pi r \cos\alpha} \tag{2.2.32}$$

Assuming no slip of the tendons, a critical bend radius giving contact between the profiles may now be determined as:

$$R_c = \frac{r}{g_1} \tag{2.2.33}$$

The contact radius for the pipe is taken as the largest $R_c$ for all helical layers. For the reason to maintain the integrity of the outer thermoplastic sheath, the manufacturers prefer to base the minimum bend radius on a permissible elongation of the outer sheath, $\varepsilon_{lim}$, which is taken as 7.5%. This gives the following limit for the bend radius:

$$R_\varepsilon = \frac{r_{out}}{\varepsilon_{lim}} \tag{2.2.34}$$

which give the following minimum bend radius for the pipe:

$$R_{min} = max(R_c, R_\varepsilon) \tag{2.2.35}$$

**Stresses in tensile layers due to bending**

- The Geodesic and the Loxodromic assumption

When slip occur between tensile layers, there are two assumptions for the slip path (see [Feret et al., 1986][3] and [Sævik, 1993][4]). One is loxodromic, and the other one is Geodesic. The loxodromic assumption describes the initial path of the slip of the each wire on the circular cylinder as if it was fixed relative to the surface, which means that it has no transverse curvature and represent a straight line on the cylinder. The geodesic assumption describes the path of the slip by the shortest distance between two points, which are respectively on the tensile and compressive sides of the pipe along the same helix.

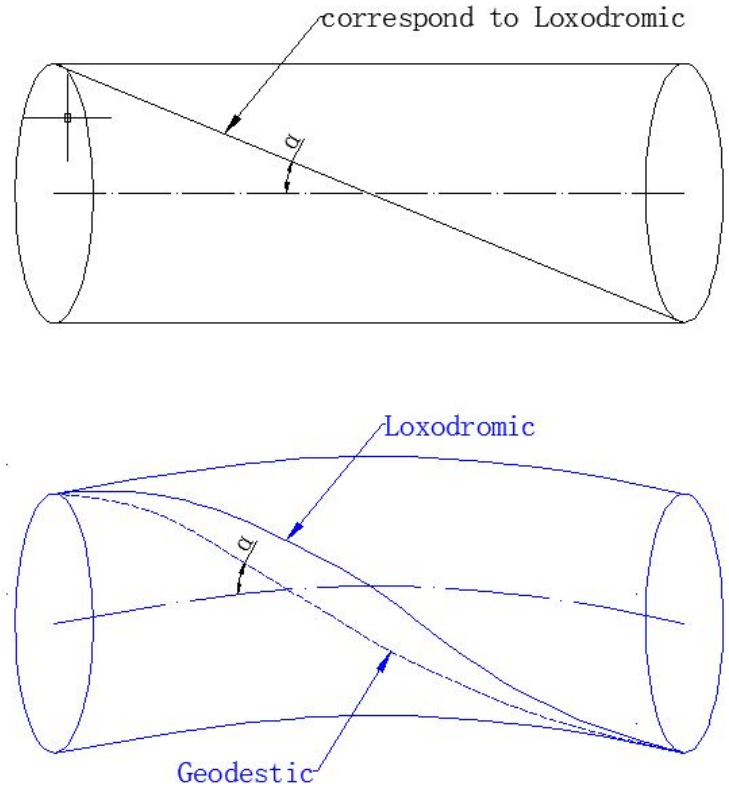


**Figure 2.9:** Definition of curve paths

**Bending stresses in tensile layers** When a pipe is bent, shear forces are created between each wire and pipe until slip occurs. However, since the axial stiffness of each wire is large relatively, longitudinal slip is enforced to eliminate the length difference between the compressive and tensile sides of the pipe, which means that the transverse slip between the wires is small relatively. Additionally, according to the work by Sævik [4], the transverse wire displacements to the geodesic will be restrained by transverse friction forces. Therefore, the dynamic bending torsion and curvature in each wire $w_{ip}$ will be between the solution of the two limited path assumption above. If no slip is assumed, loxodromic assumption applies. The following formulation can be used to determined the torsion and curvature quantities:

$$w_{1p} = \sin\alpha \cos^3\alpha \cos\psi\beta_2 \tag{2.2.36}$$

$$w_{2p} = -\cos^4\alpha \cos\psi\beta_2 \tag{2.2.37}$$

$$w_{3p} = (1 + \sin^2\alpha)\cos\alpha \sin\psi\beta_2 \tag{2.2.38}$$

Where $\beta_2$ is the global curvature at the cross-section centre and $\psi$ is the angular coordinate starting from the lower side of the pipe.

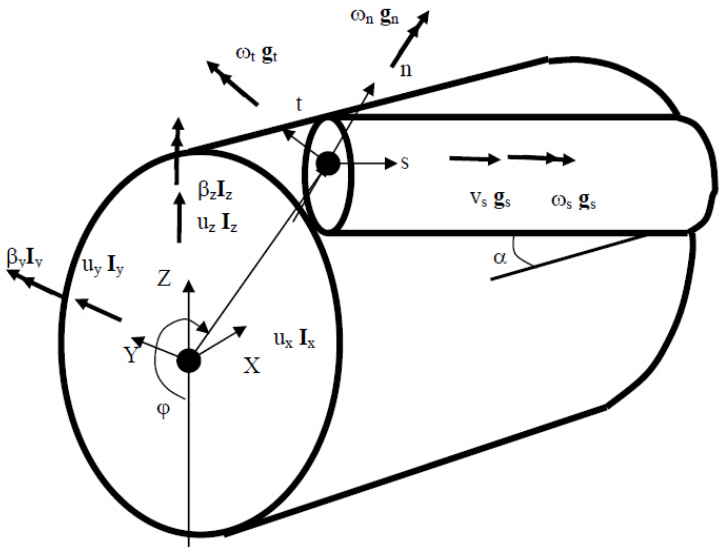


**Figure 2.10:** Definition of curvature quantities

However, as mentioned above, longitudinal slip is unavoidable, which will change the curvature quantities. If no friction is assumed, the relative displacement in longitudinal direction is given:

$$u_1 = R^2 \frac{\cos^2 \alpha}{\sin \alpha} \sin \psi\beta_2 \tag{2.2.39}$$

the torsion and the curvature are changed into:

$$w_{1p} = 2 \sin \alpha \cos^3 \alpha \cos \psi\beta_2 \tag{2.2.40}$$

$$w_{2p} = -\cos^2 \alpha \cos 2\alpha \cos \psi\beta_2 \tag{2.2.41}$$

Where it is noted that the transverse curvature is unaffected.

The quantities along the geodesic curve are:

$$w_{1p} = -\sin \alpha \cos \alpha [\frac{1}{\sin^2 \alpha - 3}] \cos \psi\beta_2 \tag{2.2.42}$$

$$w_{2p} = -3 \cos^2 \alpha \cos \psi\beta_2 \tag{2.2.43}$$

$$w_{3p} = 0 \tag{2.2.44}$$

The relative transverse displacements are given by:

$$u_2 = \frac{R^2}{\tan \alpha} [\frac{\cos^2 \alpha}{\sin \alpha} + 2 \sin \alpha] \sin \psi\beta_2 \tag{2.2.45}$$

Assuming plane deformation only occur in y plane, i.e. $\beta_2 \neq 0$. Then the axial force is

$$Q_1 = -EAR \cos^2 \alpha \cos \psi\beta_2 \tag{2.2.46}$$

By differentiation, the shear force q per unit length along the wire is obtained:

$$q_1 = EA\cos^2\alpha\sin\alpha\sin\psi\beta_2 \tag{2.2.47}$$

Normally, the maximu is found in the neutral axis of bending, which is:

$$q_{1c} = \mu(q_3^I + q_3^{I+1}) \tag{2.2.48}$$

Here $\mu$ is the friction coefficient, and $q_3^i$ is the radial line at interface i.

Set $q_1 = q_{1c}$ then the critical curvature $\beta_{2c}$ is given by:

$$\beta_{2c} = \frac{\mu(q_3^I + q_3^{I+1})}{EA\cos^2\alpha\sin\alpha} \tag{2.2.49}$$

Harmonic motion and no end effects are assumed, an arbitrary cross-section can be divided into two regions. By a angle $\psi_0$, one part of cross-section is defined as the stick domain and the other one is the slip domain. The regions are illustrated in the figure below.

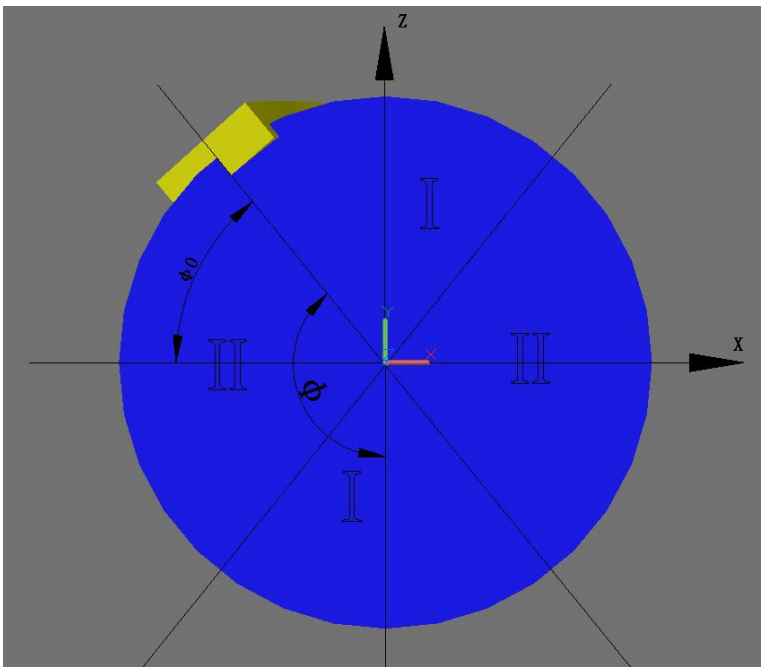


**Figure 2.11:** The definition of stick and slip domain on one cross-section

The transition between these two regions can be defined by the angle $\psi_0$

$$\psi_0 = \cos\left(\frac{\beta_{2c}}{\beta_2}\right) \tag{2.2.50}$$

The stress in the region $II$ can be expressed as:

$$\sigma_{11}(\psi) = \frac{\mu(q_3^I + q_3^{I+1})R}{\sin\alpha A}\psi \tag{2.2.51}$$

The stress in the region $I$ can be expressed as:

$$\sigma_{11}(\psi) = E\cos^2\alpha R\beta_2(\sin\psi - \sin\psi_0) + \frac{\mu(q_3^I + q_3^{I+1})R}{\sin\alpha A_t}\psi_0 \tag{2.2.52}$$

When the full slip occurs, that means $\psi = \psi_0 = \frac{\pi}{2}$, the stress in cross-section is maximum.

$$\sigma_{11} = \frac{\mu(q_3^I + q_3^{I+1})R}{\sin\alpha A}\frac{\pi}{2} \tag{2.2.53}$$

Assuming the layer as a thin layer, the bending moment can be found by integrating of the stresses. The start slip bending moment can be expressed as:

$$M_c = \frac{\mu(q_3^I + q_3^{I+1})nR^2\cos\alpha}{2\sin\alpha} \tag{2.2.54}$$

Whereas the full slip bending moment is:

$$M_c = \frac{2\mu(q_3^I + q_3^{I+1})nR^2\cos\alpha}{\pi\sin\alpha} \tag{2.2.55}$$

## 2.3 Design process

### 2.3.1 Failure modes

There are two main failure modes for non-bonded flexible pipes:

- 1. Leakage
- 2. Reduction of internal cross section

Hereby a failure mode is defined as a process which could cause the pipe system fail. The failure modes above can cause a sequence of events, which are illustrated in the figure below. Normally, the initial failure of degradation is not serious enough to lead complete failure. However, the initial failure or degradation will result in further failure or degradation which causes full failure. In API RP 17B, the initial failure or degradation is listed. The table which is shown below is one part of the whole initial failure events as an example.

Fig.(2.12) shows failure modes tree:

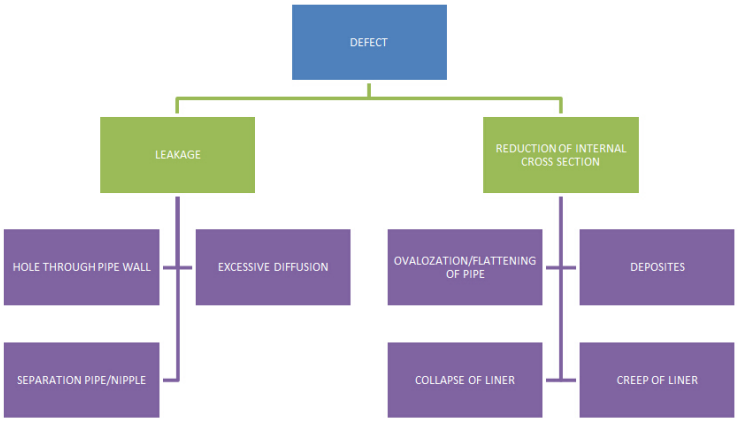


**Figure 2.12:** Failure mode tree

Fig.(2.13) shows example of potential failure modes:

| Pipe layer | Defect ref. | Defect | Consequence | Possible Cause |
|---|---|---|---|---|
| PRESSURE ARMOUR LAYER | 3.1 | Individual or multiple wire rupture | Reduced structural capacity or pipe rupture (burst) or extrusion/leakage of internal pressure sheath | a. corrosion;<br>b. SSC;<br>c. HIC;<br>d. excess internal pressure;<br>e. failure of tensile/backup pressure armour (excess tension/pressure);<br>f. unlocking;<br>g. manufacturing (welding) defect. |
| | 3.2 | Unlocking | Reduced structural capacity or pipe rupture (burst) or extrusion/leakage of internal pressure sheath | a. overbending;<br>b. excess tension;<br>c. impact;<br>d. failure of tensile or backup pressure armour;<br>e. radial compression at installation;<br>f. excess torsion during installation;<br>g. manufacturing defect (fishscaling, uncontrolled OD/pitch). |
| | 3.3 | Collapse or ovalisation | Reduced bore reduced structural capacity and collapse resistance | a. side impact;<br>b. point contact;<br>c. excess tension (in service);<br>d. radial compression at installation. |
| | 3.4 | Corrosion | Pressure armour tensile failure | a. sour service/corrosive annulus;<br>b. ingress of seawater into annulus. |

**Figure 2.13:** Example of potential failure modes

### 2.3.2 Design criteria

For non-bonded flexible pipes, several design criteria have to be met. These criteria are mainly:

**1. Strain** For internal sheath and outer sheath, strain is an important design criterion. The allowable strains for materials are recommended in API SPEC 17J. The allowable strains are verified by materials test related to service, ageing conditions and historical field performance.

**2. Creep** When determining the wall thickness of internal pressure sheath, one should be counted is creep. There are two main methods to design the wall thickness: 1. Physical tests 2. Finite element analyses, calibrated with gap span test data In API SPEC 17J, there are specified layer creep design criteria based on the methods above.

**3. Stress** Safety factors are given when designing stress. These factors prescribe that the maximum allowable average layer stress as proportional function of structural capacity

of steel material.

**4. Hydrostatic collapse** Factors related to hydrostatic buckling is given in API SPEC 17J. Hydrostatic collapse calculation should be performed for both an intact outer sheath and a breached outer sheath. During the calculation, the minimum value of the two hydrostatic pressures is taken as the hydrostatic resistance. When calculating the hydrostatic resistance, an initial ovalization has to be assumed.

**5. Mechanical collapse** When designing against to mechanical collapse, one should consider is that the contribution of steel layers act as the support of carcass. Utilization factors related to this is specified in API SPEC 17J.

**6. Torsion** When deriving the maximum acceptable torsion, we consider two load scenarios: 1. The outer tensile armour layer is turned inward and pressed against the internal layer 2. The outer tensile armour layer is turned outward and pressed again the external layers

**7. Crushing stress and ovalization** The collapse load due to crushing stress and ovalization should be calculated by combining the resistance of the internal carcass and pressure layers which act as the support of carcass. There are also two alternative methods recommended for calculation of the collapse due to crushing stress and ovalization: 1. Finite element analysis 2. Analytical/empirical formulae The compressive radial loads and axial loads induced by the installation procedure should limited such that the design criteria specified for installation are met. In particular, the maximum allowable installation tension should be established as the value that meets the applicable criteria. Additionally, the maximum permanent ovalisation of the pipe for both installation methods should be less than the value of initial ovalisation used for hydrostatic collapse calculations.

**8. Compression** Criteria related to compression are specified in API SPEC 17J. When the compression has to be checked, we should investigate the maximum compression. The maximum compression should be in the range of the criteria in API SPEC 17J.

**9. Service life factors** The design service life differs in different projects, replacement programs. Thus, we have to give some considerations regarding to service life or replacement of components. Additionally, the fatigue calculation regarding to service life are specified in API SPEC 17J.

# Chapter 3

# Numerical Solution

## 3.1 General

Three models for 6inch, 8inch and 16inch flexible pipes are built and modeled in BFLEX. BFLEX is a program system for analysis of extreme stresses and fatigue in the tensile- and pressure armour layers of flexible pipes. The system includes two main components:

- BFLEX Analysis Modules (BFLEX, PFLEX, LIFETIME, BOUNDARY, TEMPERATURE).
- FEM/RAF Result Database.

An overview of BFLEX program system is illustrated:

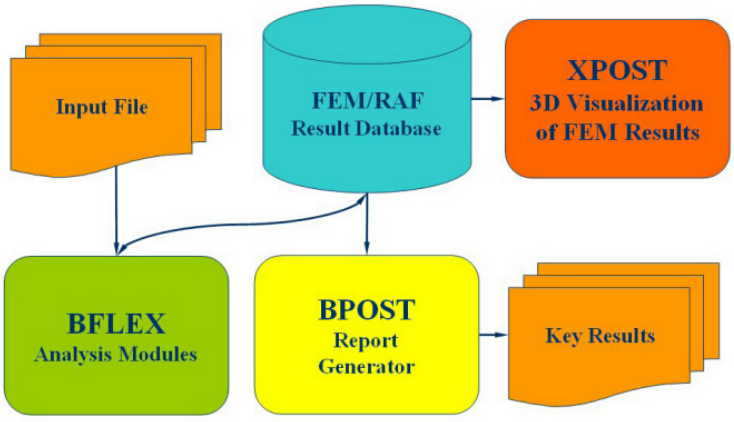


**Figure 3.1:** An overview of BFLEX program system

The BFLEX analysis modules currently include the following functionality:

- The BFLEX module, reading and controlling all input data needed for all modules, and performing tensile armour stress analysis.
- The PFLEX module, performing pressure spiral bending stress analysis.
- The LIFETIME module, performing fatigue analysis.
- The LIFETIME module, performing fatigue analysis.
- The TEMPERATURE module, performing temperature analysis.

In modelling, for ITCODE31, element PIPE52 is used to model all the metallic layers.

| **Layer name** | **Element type** | **Explanation** |
|---|---|---|
| core | PIPE52 | core element group which includes carcass , pressure armour and plastic layers |
| tensile1 | PIPE52 | inner first tensile layer group |
| tensile2 | PIPE52 | inner second tensile layer group |

**Table 3.1.1:** Element type used in ITCODE31 model

The model based on ITCODE31 consists of 20 elements in each layers and 3 element groups.

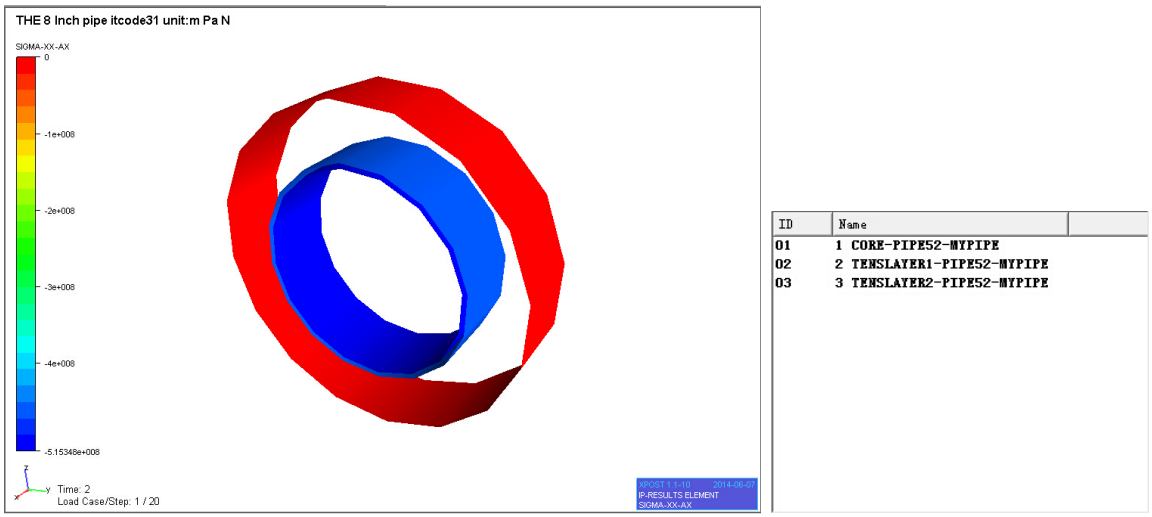


**Figure 3.2:** An ITCODE31 model in BFLEX program

For ITCODE0, element PIPE52 is used for carcass layer and zeta layer meanwhile HSHEAR352 is used for tensile layer;

| **Layer name** | **Element type** | **Explanation** |
|---|---|---|
| core | PIPE52 | core element group which includes carcass , pressure armour and plastic layers |
| tensile1 | HSHEAR352 | inner first tensile layer group |
| tensile2 | HSHEAR352 | inner second tensile layer group |

**Table 3.1.2:** Element type used in ITCODE0 model

The model based on ITCODE0 consists of 20 elements in each layers and 3 element groups.

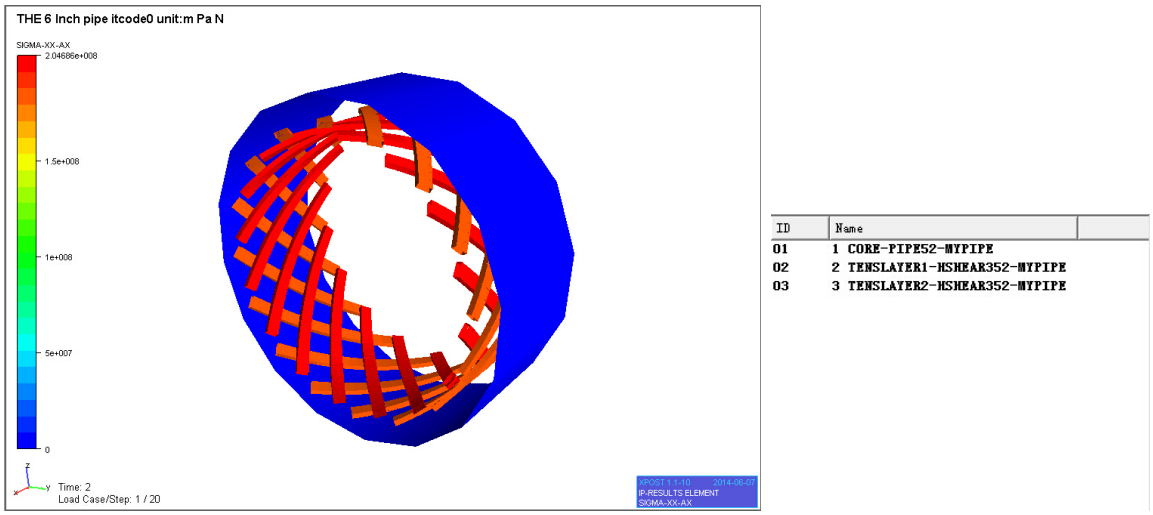


**Figure 3.3:** An ITCODE0 model in BFLEX program

For full finite element model, element HSEAR363, HSHEAR353 and HCONT463 are used, and among them, HSHEAR363 is used to model carcass and zeta layers, HSHEAR353 is for tensile layers, HCONT463 is for contact layers.

| Layer name | Element type | Explanation |
|---|---|---|
| carcass | HSHEAR363 | interlocked carcass layer |
| seal | HSHEAR363 | plastic layer between carcass and pressure armour |
| zeta | HSHEAR363 | pressure armour |
| structape | HSHEAR363 | plastic layer between pressure armour and tensile layer |
| contactseal | HCONT463 | contact layer between plastic layer and tensile layer |
| tensile1 | HSHEAR353 | inner first tensile layer group |
| tapeoutwardcontact | HCONT463 | contact layer between two tensile layers |
| tapeinwardcontact | HCONT463 | contact layer between two tensile layers |
| tensile2 | HSHEAR353 | inner second tensile layer group |
| sheathcontact | HCONT463 | contact layer between second tensile layer and outersheath |

**Table 3.1.3:** Element type used in full FE model

More element group is specified in full Fe model since every layer is defined separately.

The model consists of 20 elements in each layers and 11 element groups.

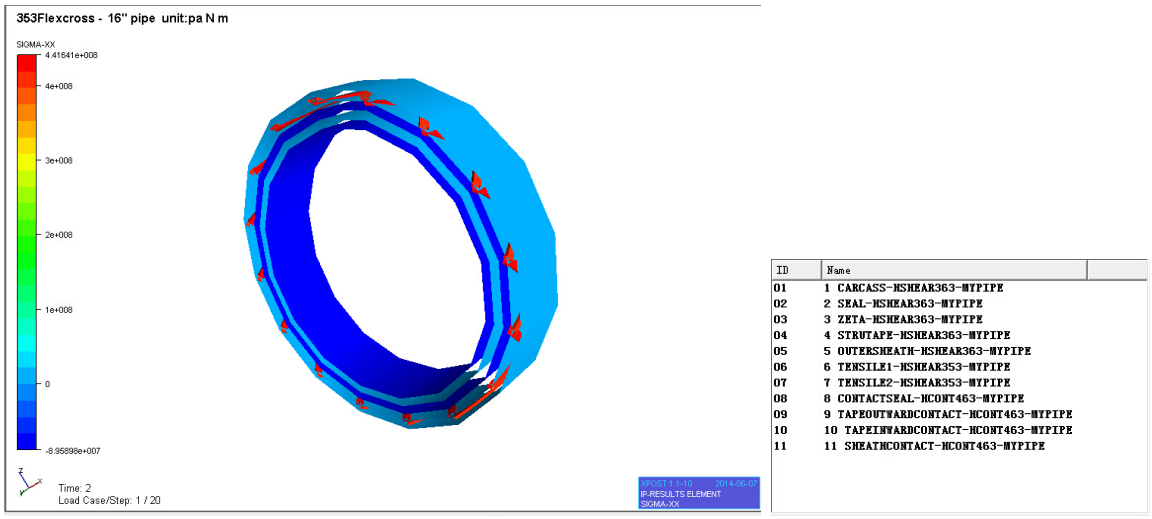


**Figure 3.4:** An full FE model in BFLEX program

## 3.2 ITCODE31 and ITCODE0

### 3.2.1 General

For ITCODE31, all metallic layers are modelled by element PIPE52. According to BFLEX user manual [5] and BFLEX theory manual [6], the PIPE52 beam element is a 2 noded 12 dof element used to model flexible pipes, and serves several purposes:

- Model the bending stiffener.
- Model the axisymmetric and bending contribution from a flexible pipe.

### 3.2.2 Axisymmetric Model and Formulation

According to work done by Custodio and Vaz [7], several most common assumptions were listed for the axisymmetric model

- 1. Regularity of initial geometry: (a) the homogenous layers are ling and uniform cylinders; (b) the wires are wound on a perfectly cylindrical helix; (c) the wires are equally spaced; (d) the wires of an armour are numerous, hence the forces they exert on the adjacent layers may be replaced by uniform pressure; (e) the structure is straight.

- 2. Reduction to simple plane analysis: (f) there are no field loads such as self-weight; (g) end effects may be neglected; (h) the material points from any layer has same longitudinal displacement and twist; (i) all wires of an armour present the same stress state; (j) the wires maintain a helicoidal configuration when strained; (k) the angle between the wire cross-section principal inertia axis and a radial vector linking the centre of structure's cross-section and the centre of wire's cross-section is constant; (l) there is no over-penetration or gap spanning.
- 3. The effects of shear and internal friction are neglected: (m) the wires are so slender that the movements of the material points are governed only by their tangent strain and not by the change in curvature.
- 4. Linearity of the response: (n) the materials have linear elastic behaviour; (o) the changes in armour radius and pitch angles are linearly small; (p) the wires in one armour never touch laterally or are always in contact; (q) there are no voids between layers; (r) the homogeneous layers are thin and made of soft material so they simply transfer pressure; (s) the pipes's core responds linearly to axisymmetric loading; (t) both loading and response are not time-dependent.

The model is based on assumption (a)-(t), except (p) and (m) where the effect of gap closure in the circumferential direction and change in curvature are included. This is to allow the model to be applicable for umbilicals as well, where circumferential contact is known to occur and where the bending sitffness contirbution from each component may be significant. The model is threrfore cosiderd applicable for both umbilicals and flexible pipes exposed to stresses within the elastic range.

The strain-stress relation in wires is given as:

$$\varepsilon_1 = u^0_{1,1} - \kappa_3 u^0_2 + \kappa_2 u^0_3 \tag{3.2.1}$$

$$\varepsilon_2 = u^0_{2,1} + \kappa_3 u^0_1 + \kappa_1 u^0_3 \tag{3.2.2}$$

$$\varepsilon_3 = u^0_{3,1} - \kappa_2 u^0_1 + \kappa_1 u^0_2 \tag{3.2.3}$$

**Tendon contribution** According to the work of Sævik[8] and J.A.Witz & Z.Tan[9], based on equilibrium of an infinitesimal segment considering the differentials of both stress resultants and base vectors as illustrated below, there are six differential equations defined and describing the equilibrium of the curved tendon. For axisymmetric model, the assumption of cylindrical deformation implies that the strain field has to be constant and that all terms related to $k_3$ are zero, which means that only two equations remain:

$$-\kappa_2 Q_1 + \kappa_1 Q_2 + q_3 = 0 \tag{3.2.4}$$

$$-\kappa_2 M_1 + \kappa_1 M_2 + Q_2 = 0 \tag{3.2.5}$$

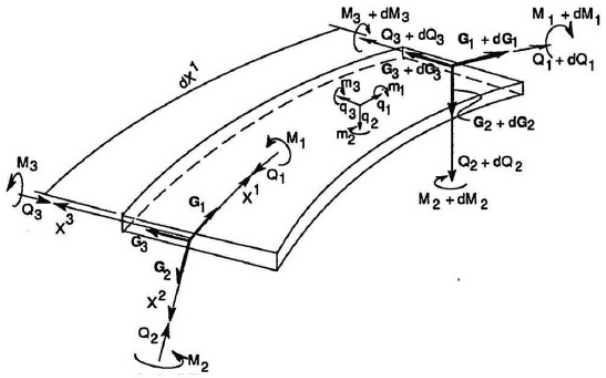


**Figure 3.5:** Illustration of beam element

DOFs at the cross-section centre and the radial displacements DOFs for each layer in the following way. First, the kinematic constraint is introduced:

$$\theta_1 = -\kappa_t u_2 + \kappa_1 u_1 \tag{3.2.6}$$

The kinematic constraint equation was found to govern prestressed tensile armour behaviour in the work of Sævik[2]. It also used to prove the link between curvatures and displacements for the loxodromic and geodesic limit curves on the pipe surface. The transverse curvature of the cylinder surface $\kappa_t$ is obtained by the equation of Euler:

$$\kappa_t = \cos\alpha^2 \kappa_r + \sin\alpha^2 \kappa_c \tag{3.2.7}$$

Where $\alpha$ is the helix lay angle and where $\kappa_r$ and $\kappa_c$ represent the principal curvatures in the circumferential and longitudinal directions of the cylinder surface. The above means that the rotation around the $X^1$-axis is given by the axial and transverse displacements directly. Further, the components of helix deformation due to axisymmetric loads are given by:

$$u_1 = \omega_1 \cos\alpha + R \sin\alpha \chi_1 \tag{3.2.8}$$

$$u_2 = \omega_1 \sin\alpha - R \cos\alpha \chi_1 \tag{3.2.9}$$

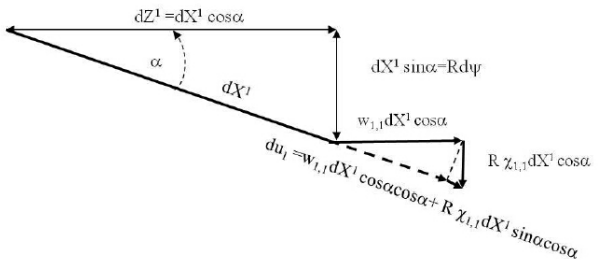


**Figure 3.6:** Axisymmetric deformation quantities

Where $R$ is the layer mean radius. Noting that $Z_1 = X_1 \cos\alpha$, that $\kappa_2 = \frac{\sin\alpha^2}{R}$ along circular helix and that $\kappa_c = 0$ along the straight cylinder, the governing contributions to the Green strain for the helix can be expressed by differentiation with respect to $Z^1$ as:

$$\varepsilon_1 = \cos\alpha^2 \omega_{1,1} + \frac{\sin\alpha^2}{R} u_3 + R \sin\alpha \cos\alpha \chi_{1,1} \tag{3.2.10}$$

$$\omega_1 = \frac{\sin\alpha^3 \cos\alpha}{R} \omega_{1,1} - \frac{\sin\alpha^3 \cos\alpha}{R^2} u_3 + \cos\alpha^3 \chi_{1,1} \tag{3.2.11}$$

$$\omega_2 = -\frac{\sin\alpha^2\cos\alpha^2}{R}\omega_{1,1} + \frac{\sin\alpha^2\cos\alpha^2}{R^2}u_3 + (2\sin\alpha\cos\alpha^3 + \sin\alpha^3\cos\alpha)\chi_{1,1} \quad (3.2.12)$$

Where $_{,1}$ here means differentiation with respect to $Z_1$ and $\omega_1$ and $\chi_1$ represents the common axial and torsion DOFs at the centroid of the cross-section and $u_3$ represents the radial DOF necessary to describe the radial motion of each layer which in turn may result in gaps between layers.

The radial gap at interface I is initially assumed to be zero and can for any equilibrium state with reference to Fig.(3.7) be expressed by:

$$g_3^I = (R+u_3)^{I+1} - (R+u_3)^I - \frac{(t+\Delta t)^{I+1}}{2} - \frac{(t-\Delta t)^I}{2} \quad (3.2.13)$$

Where $t$ is the thickness of the tendon and thickness reduction is taken to be positive. If $g_3^I = 0$ the radial strain $E_{33}$ for layer I can be expressed as:

$$E_{33} = -\frac{\Delta t}{t} \quad (3.2.14)$$

The axisymmetric model used in BFLEX is illustrated in following figure.

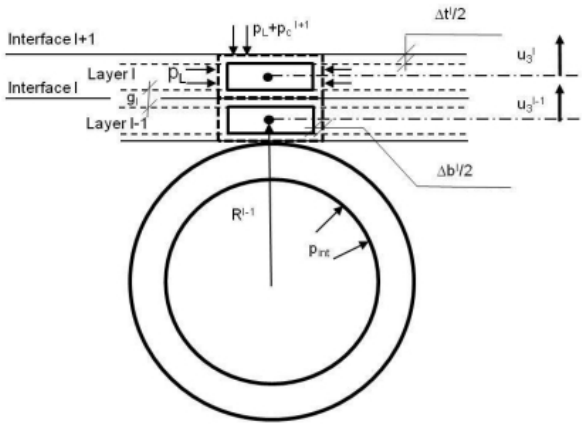


**Figure 3.7:** An axisymmetric layer model

The contact pressure at interface I is linked to the tendon radial stress $S_{33}$ in layer I by the relation:

$$p_3 = -F_f S_{33} = F_f \frac{q_3}{b} \tag{3.2.15}$$

where b is the width of each tendon and the fill factor $F_f$ is dened by:

$$F_f = \frac{nb}{2\pi R \cos\alpha} \tag{3.2.16}$$

where n is the number of tendons in the layer. The contact pressure further consists of to components:

$$p_3 = p_L + p_{3c} \tag{3.2.17}$$

$p_L$ is a local prescribed pressure and pc represents the contact pressure due to the layer external load reactions. If g $>$ 0 then $p_c = 0$ and p $= p_L$. At interface no. 1, $p_L$ equals the internal pressure whereas for interface n+1, $p_L$ normally equals the external pressure. However, in the case of damaged outer sheath, all layers outside the rst watertight sheath will be exposed to the same local (external) pressure.

For ITCODE0, carcass and zeta layers are modelled by element PIPE52 meanwhile helical tensile layers are modelled by element HSHEAR352.
According to BFLEX user manual [5] and BFLEX theory manual [6], element HSHEAR352 is a 4 noded 16 dof curved sandwich beam element used to model helical tensile layers. It includes 12 beam dofs corresponding to those of pipe31 plus 4 helical DOFS along the helix, allowing longitudinal slip to be modelled.

The axisymmetric models used for element HSHEAR352 is same with the model applied for ITCODE31 case.

## 3.3 Full Finite Element

### 3.3.1 General

For full finite element model, element HSEAR363, HSHEAR353 and HCONT463 are used, and among them, HSHEAR363 is used to model carcass and zeta layers, HSHEAR353 is for tensile layers, HCONT463 is for contact layers.
According to BFLEX user manual [5] and BFLEX theory manual [6], element HSHER353 is a 4 noded 26 dof curved beam element dedicated to the modelling of helices. It includes 12 beam dofs corresponding to those of PIPE31 plus 6 helical DOFS at each end of the corresponding helix. In addition 2 two internal dofs are used to allow accurate description of the longitudinal slip process. Element HSHEAR363 is a 4 noded 18 dof beam-shell element dedicated to the modelling of the pressure armour, the anti-buckling tape and the plastic layers.It includes 12 beam dofs corresponding to those of PIPE31 plus 3 dofs associated to separate nodes having the same geometric location as the end beam nodes. Element HCONT463 is a 4 noded hybrid mixed contact element used to connect the hshear elements to the core and to describe contact between the HSHEAR elements.

### 3.3.2 Element models

#### HCONT353

[6]The finite element model normally includes six beam degrees of freedom per node. The standard beam elements includes two nodes. However for the HSHEAR353 elements additional nodes are introduced to allow the motion being described as a sum of standard beam quantities that describe the plane surfaces remain plane condition and the relative deformations resulting from slip.

By neglecting shear deformations including end section warping and only considering the motion of the helix centre line, the kinematic quantities governing the longitudinal strain was formulated by Sævik[8]. The quantities of relevance here are with reference to Fig.(3.8) as:

$$GE_{11} = \epsilon_1 + X^3\omega_2 - X^2\omega_3 + \frac{1}{2}\epsilon_1^2 + \frac{1}{2}\epsilon_2^2 + \frac{1}{2}\epsilon_3^2 \tag{3.3.1}$$

Where:

$$\varepsilon_1 = u_{1,1} - \kappa_3 u_2 + \kappa_2 u_3 \tag{3.3.2}$$

$$\varepsilon_2 = u_{2,1} + \kappa_3 u_1 - \kappa_1 u_3 \tag{3.3.3}$$

$$\varepsilon_3 = u_{3,1} - \kappa_2 u_1 + \kappa_1 u_2 \tag{3.3.4}$$

$$\omega_1 = \kappa_1 u_{1,1} - \kappa_t u_{2,1} + \kappa_3(u_{3,1} + \kappa_1 u_2) + \kappa_2(u_{2,1} - \kappa_1 u_3) + \omega_{1p} \tag{3.3.5}$$

$$\omega_2 = -u_{3,11} + \kappa_2 u_{1,1} - 2\kappa_1 u_{2,1} - \kappa_3\kappa_t u_2) + \kappa_1\kappa_1 u_3 + \omega_{2p} \tag{3.3.6}$$

$$\omega_3 = u_{2,11} + \kappa_3 u_{1,1} - 2\kappa_1 u_{3,1} + \kappa_2\kappa_t u_2) - \kappa_1\kappa_1 u_2 + \omega_{3p} \tag{3.3.7}$$

$u_{i,j}$ denotes differentiation of the displacement components $u_i$ along axes $X^i$ with repect to the curve linear coordinate $X^j$. $E_{11}$ is the Green strain tensor in curve linear coordinate, $G$ is the metric, $\epsilon_1$ represents the $1^{st}$ order axial strain, $\epsilon_2$ is the centre line rotation about the $X^3$ axis, $\epsilon_3$ is the centre line rotation about the $X^2$ axis, $\omega_i$ is the centre line torsion, $\omega_2$ is the curvature about the $X^2$ axis and $\omega_3$ is the curvature about the $X^3$ axis. The $\omega_{ip}$ quantities represents the prescribed torsion and curvature quantities from bending whereas the $\kappa_i$ quantities represents the initial torsion and curvatures. It is also noted that in these expressions the convention of positive torsion and curvature are based on obtaining positive rotation when moving an unit distance along the $X^1$ axis. Further, in the initial helix state from which $\omega_i$ and $\epsilon_i$ are measured, $\kappa_1 = \frac{\sin\alpha\cos\alpha}{R}$, $\kappa_2 = \frac{\sin\alpha^2}{R}$ and $\kappa_3 = 0$. For thick helix elements the effect of the metric becomes significant and should

be included when calculating stresses.

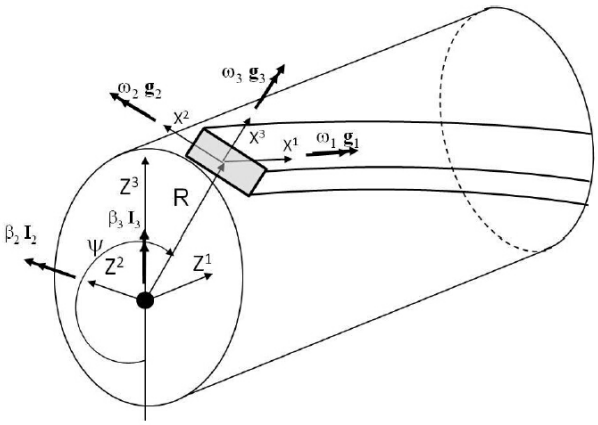


**Figure 3.8:** Kinematic quantities and coordinate system

It is noted that the above includes the kinematic constraint describing the torsion rotation $\theta_1$ as:

$$\theta_1 = \kappa_1 u_1 - \kappa_t u_2 \tag{3.3.8}$$

which assumes that the wire is forced to follow the supporting surface, from (Sævik,1993)[4] having a variable transverse curvature $\kappa_t$ given by:

$$\kappa_t = \frac{\cos\alpha^2}{R} + \sin\alpha^2\left(\frac{-\omega_{2,11}\sin\psi}{1 - R\omega_{2,11}\sin\psi} + \frac{\omega_{3,11}\cos\psi}{1 + R\omega_{3,11}\cos\psi}\right) \tag{3.3.9}$$

Where $\omega_i$ is the global displacement along the global axis $Z^i$

The prescribed quantities $\omega_{ip}$ are obtained as:

$$u_{1p,1} = R\cos\alpha^2\cos\psi\omega_{3,11} - R\cos\alpha^2\sin\psi^2\omega_{2,11} + \cos\alpha^2\omega_{1,1} + R\cos\alpha\sin\alpha\chi_{1,1} \tag{3.3.10}$$

$$\omega_{1p} = \sin\alpha\cos\alpha^3(-\cos\psi\omega_{3,11} + \sin\psi\omega_{2,11}) + \frac{\sin\alpha^3\cos\alpha}{R}\omega_{1,1} + \cos\alpha^4\chi_{1,1} \tag{3.3.11}$$

$$\omega_{2p} = \cos\alpha^4(\cos\psi\omega_{3,11} - \sin\psi\omega_{2,11}) - \frac{\sin\alpha^2\cos\alpha^2}{R}\omega_{1,1} + (2\sin\alpha\cos\alpha^3 + \sin\alpha^3\cos\alpha)\chi_{1,1} \tag{3.3.12}$$

$$\omega_{3p} = (1 + \sin\alpha^2)\cos\alpha(-\sin\psi\omega_{3,11} - \cos\psi\omega_{2,11}) \tag{3.3.13}$$

Where $\chi_i$ represent the prescribed rotation quantities at the pipe centreline illustrated in Fig.(3.8) which defines the DOFs needed for the new element. The element now includes all together 26 degrees of freedom, 12 are associared to the standard beam dofs of the centreline to describe the prescribed global strain quantities whereas 14 is applied to describe the local displacement of the wire relative to the core. This allows qubic interpolation in all directions, thus circumventing membrane locking phenomena due to the curvature coupling terms.

**HCONT463**

The HCONT463 element is developed to fit the quantities as defined for the HSHEAR353 and HSHEAR363 beam elements. Both the longitudinal $X^1$ and transverse $X^2$ and $X^3$ directions are included for the HSHEAR353 end of the element whereas for the HSHEAR363 end only the radial displacement field is considered. Fig.(3.9) shows that two elements A and B may come into contact. The displacements along the helix beam HSHEAR353 side includes the radial displacement and is described by 4DOFs whereas the HSHEAR363 side includes 6 DOFs which gives 10 DOFs in total. To make it march the srandard 6 dofs in each node, the element is implemented with 18 dofs where the torsion dof is dummy.

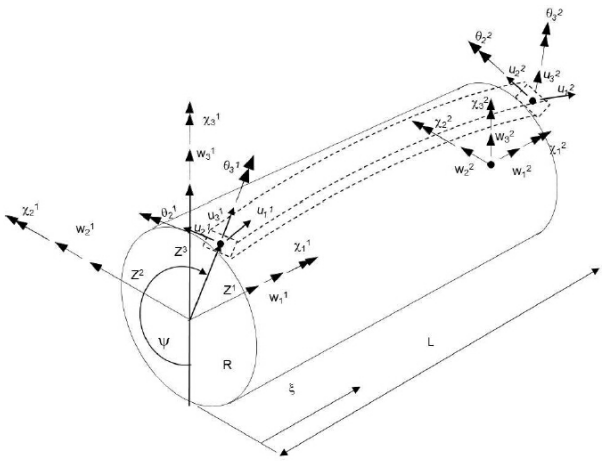


**Figure 3.9:** HCONT463 element with 10 degree of freedom

Considering two beam elements A and B, the contact kinematics can be expressed as:

$$\Delta u_n = (\Delta \mathbf{u}_B - \Delta \mathbf{u}_A)\cdot = (\Delta u_3^{0B} - \Delta u_3^{0A}) \tag{3.3.14}$$

Where:

$$\Delta u_3^{0A} = (1-\xi)u_3^1 + \xi u_3^1 - L\xi(1-\xi)^2 - L\xi^2(1-\xi) \tag{3.3.15}$$

$$\Delta u_3^{0B} = (\gamma_1^1 + \gamma_2^1 \cos 2\psi(1-\xi) + (\gamma_1^2 + \gamma_2^2 \cos 2\psi + \gamma_3^2 \sin 2\psi)\xi \tag{3.3.16}$$

# Chapter 4

# Modelling Method

## 4.1 General

Three load cases which denote tension-only, internal pressure-only, and external pressure only cases were applied to each of three flexible pipes. During the modelling, for all of pipes, the introduced tension was controlled to increase linearly from 0 to 3000KN. Same control is applied to internal pressure-only and external pressure-only cases, and the peak values both for introduced internal and external pressure were 20MPa.

## 4.2 Tension-only case

In this case, the flexible pipe is modelled as that a part of pipe lies on the sea bottom and tension is the only load the pipe subjected. A short model is built in BFLEX to avoid the free spanning effects. The introduced tension is acting on the carcass layer. The boundary condition for the pipe is illustrated below. All 6 DOFs at one end of the pipe are fixed meanwhile only DOF in longitudinal direction is free to displace at the other end. Both two ends are modelled as simple supports.


**Figure 4.1:** Boundary conditions for the model

Since the pipe is modelled to subject tension only, there is no need to perform dynamic analysis and fatigue analysis. Therefore, to reduce the computing time and work efficiently, a short analysis time which is 2s is applied to the model. Additionally, to simplify the modelling, the plastic layers between metallic layers is merge to be one thick plastic layers, which means that there is only one plastic layers between two metallic layers. For ITCODE31 and ITCODE0, carcass model, pressure armour and plastic layers are in one group named core which is modelled by PIPE52 element whereas these layers are modelled by HSHEAR363 element in different groups for full FE model. The effect due to this difference will be discussed in next chapter. Additionally, for full FE model, one should be noted is that carcass, pressure armour and plastic layer between them are merged to one coordinate system, which means that these three layers will behave as a whole when modelling. Moreover, for full FE model, contact layers which are modelled by HCONT463 element are introduced to model the effects between each two layers.

## 4.3 Internal pressure-only case

For internal pressure acting only case, similarly, short simplified models are built for the case and same boundary conditions are applied. As mentioned previously, all layers of carcass, pressure armour and plastic are defined in one group for ITCODE31 and ITCODE0. For those two models, internal pressure can be simply introduced. For full FE model, layers are defined in separated groups. Since it is expected that the axial stress in carcass layer is negligible, the controlled internal pressure is introduced at the seconde layer (inside-out order) of the pipe, that is, the plastic layer between carcass and pressure armour. However, due to the gap effect between carcass and the next plastic

layer, convergence is not obtained if the internal pressure is acting on the plastic layer. Considering that carcass doesn't take any axial stress when subjected internal pressure, a modification that fixed both two ends of carcass layer is applied. Compared to tension-only case, carcass is in another independent coordinate system.

## 4.4 External pressure-only case

For external pressure-only case, short simplified models and same boundary conditions are applied again. In this case, external pressure is introduced on the outersheath. Since the model built in BFLEX is a simplified model, that is, plastic layers between two metallic layers is summed, it results in that there is one thick layer outside the pipe. When modelling the thick outside layer takes more stress than it actually does, introducing significant effect to the results. To minimize the effect, based on the model applied for tension-only case, one modification is that the original thick outersheath is divided into two layers which are consist of one inside thick layer and one outside thin layer.

## 4.5 Analytical solution

### 4.5.1 General

Analytical solution here is based on recommended formulation in Handbook on Design and Operation of Flexible Pipes [10]. The analytical solution is for a rough estimation to evaluate the computing result, therefore full calculation was not performed and the accuracy of the analytical solution is on low sides.

### 4.5.2 Tension-only case

The following equations are used to calculate the stress:

$$\sum n_i \sigma_i A_i \cos \alpha_i = T_w = T_e \tag{4.5.1}$$

Where

$T_e$ denotes the control tension which is introduced to model. By the equation, true wall force $T_w$ is found.

Axial stress in tensile layers are:

$$\sigma_t = \frac{T_w}{nA_t \cos\alpha} \tag{4.5.2}$$

where n is the total number of tendons in the armouring layers, $A_t$ is the cross section area of the tendon, t is the total thickness of the tensile armours. $\alpha$ denotes the lay angle of the helical tensile layers.

For the axial stresses in carcass and pressure armour, contact pressure between pressure armour and tensile layer is calculated:

$$P_T = \frac{T_w tg^2\alpha}{2\pi r^2} \tag{4.5.3}$$

According to equilibrium:

$$\sigma_{xx} = -\frac{\overline{R}^{c+z}}{t_{eff}} P_T \tag{4.5.4}$$

Where

- $\overline{R}^{c+z}$ denotes the mean radius of carcass and pressure armour (zeta shape profile).

- $t_{eff}$ denotes the total effective thickness of carcass and pressure armour.

The following equations are used to calculate effective thickness $t_{eff}$:

$$t_{eff} = \frac{nA}{L_p} \tag{4.5.5}$$

$$\text{Ł}_p = \frac{2\pi R}{\tan\alpha} \tag{4.5.6}$$

$L_p$ denotes the pitch length of the layer and n is the number of tendon of the layer.

In this way, axial stresses of carcass and pressure armour can be calculated. However, it is assumed that carcass and pressure armour are merged to one when calculating by this way, therefore the axial stress in carcass equals to pressure armour. The reason for the assumption is that carcass and pressure armour is in the same coordinate system and behave together in BFLEX model for tension-only case. Besides, the analytical solution is a rough estimation without high accuracy requirement.

### 4.5.3 Internal pressure-only case

For internal pressure-only case, true wall force $T_w$ is determined by:

$$\sum n_i \sigma_i A_i \cos \alpha_i = T_w = \pi P_{int} r_{int}^2 \tag{4.5.7}$$

Where

$P_{int}$ denotes the introduced internal pressure in BFLEX. $r_{int}$ is the radius of internal pressure.
Afterwards the axial stress in tensile layer can be found by Eq.(4.5.2).

Contact pressure for internal pressure-only case also can be found by Eq.(4.5.3). It is expected that carcass almost doesn't take any created load, therefore, according to equilibrium, the axial stress in pressure armour are:

$$\sigma_{xx} = \frac{\overline{R}^z}{t_{eff}^z}(P_{int} - P_T) \tag{4.5.8}$$

Where

$t_{eff}^z$ denotes the effective thickness of pressure armour.

### 4.5.4 External pressure-only case

For external pressure-only case, true wall force is found by:

$$\sum n_i \sigma_i A_i \cos \alpha_i = T_w = \pi P_{ext} r_{ext}^2 \tag{4.5.9}$$

Where

$P_{ext}$ denotes the introduced external pressure in BFLEX. $r_{ext}$ is the radius of external pressure.

The axial stress in tensile layers is found by Eq.(4.5.2) similarly after $T_w$ is found.

The contact pressure:

$$\sigma_{xx} = \frac{\overline{R}^z}{t_{eff}^{c+z}}(P_{ext} - P_T) \tag{4.5.10}$$

# Chapter 5

# Numerical Studies

## 5.1 Tension-only case

### 5.1.1 Axial stress in carcass and pressure Armour

The axial stress in carcass and pressure armour for 6inch flexible pipe is illustrated below:

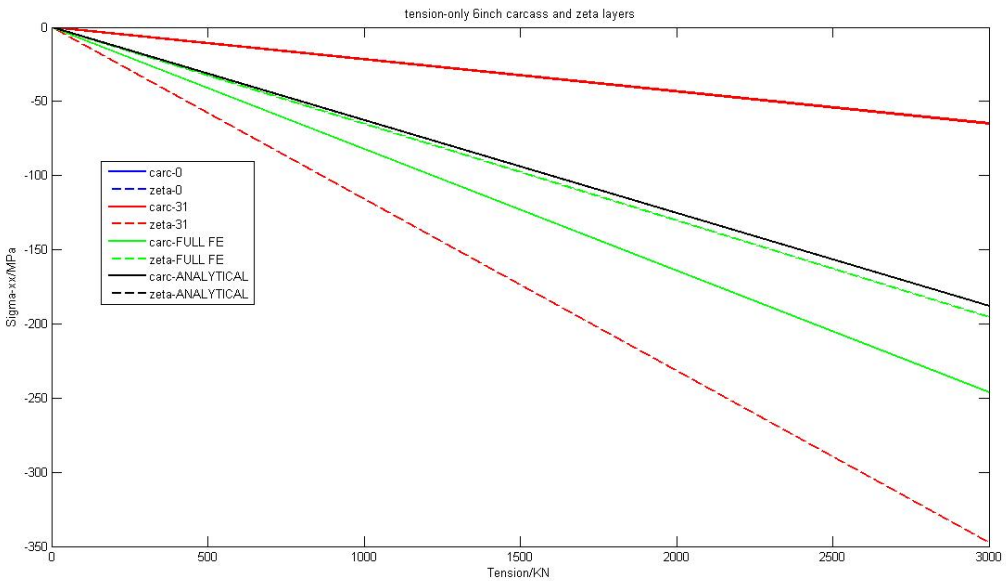


**Figure 5.1:** 6inch flexible pipe stress distribution in carcass and pressure armour for tension-only case

The axial stress in carcass and pressure armour for 8inch flexible pipe is illustrated below:

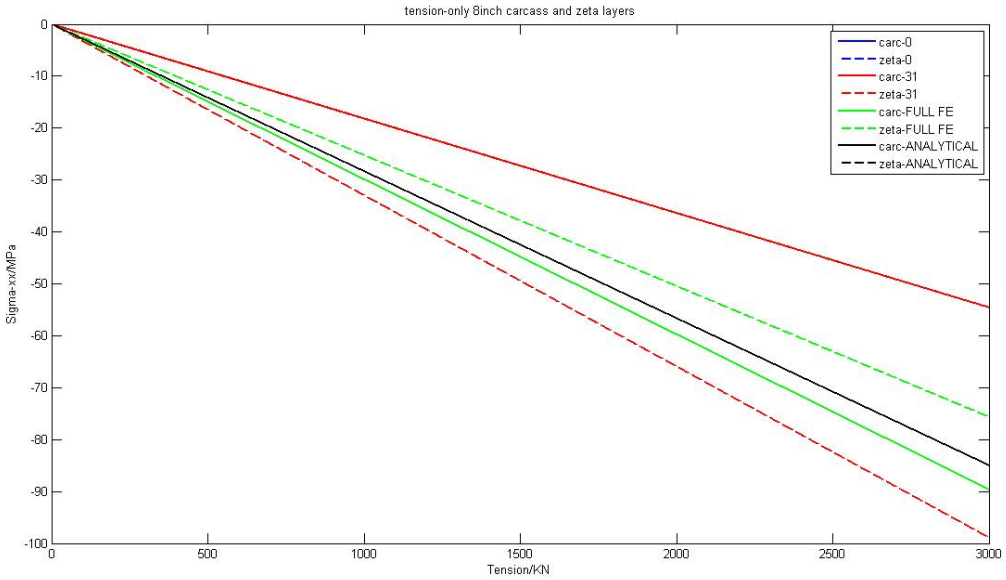


**Figure 5.2:** 8inch flexible pipe stress distribution in carcass and pressure armour for tension-only case

The axial stress in carcass and pressure armour for 8inch flexible pipe is illustrated below:

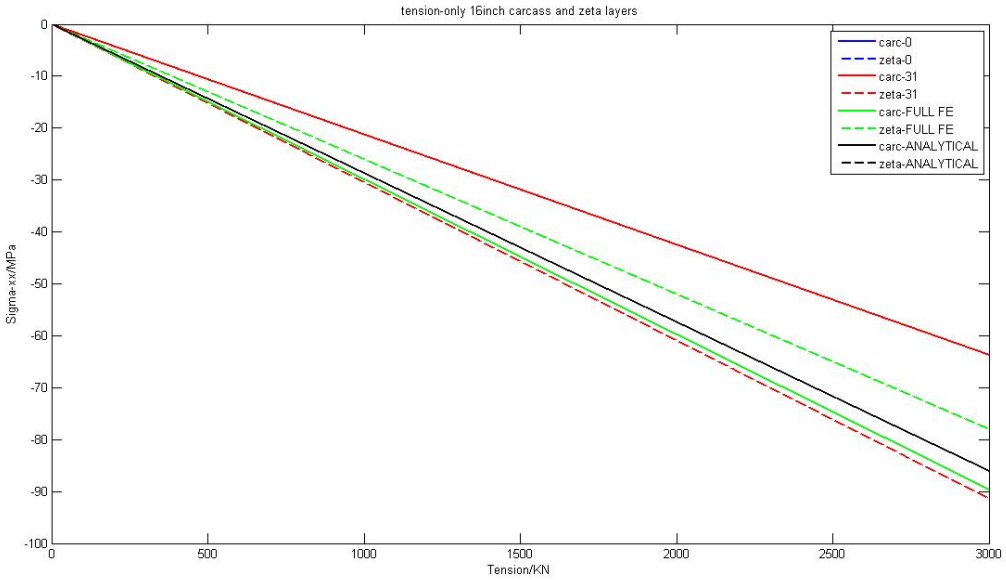


**Figure 5.3:** 16inch flexible pipe stress distribution in carcass and pressure armour for tension-only case

For comparison, merge three figures into one and extract the peak values for each model and analytical solution:

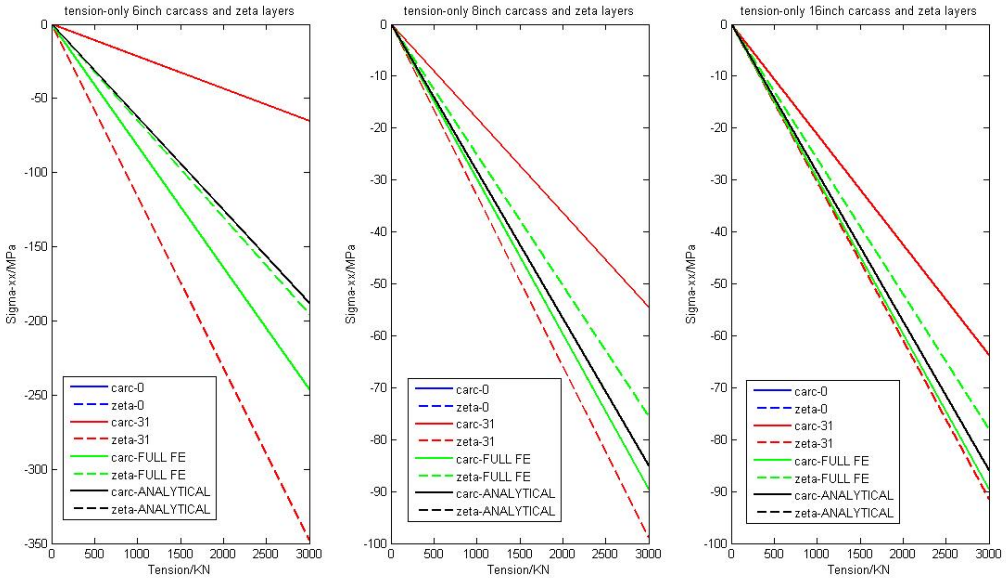


**Figure 5.4:** Stress distribution in carcass and pressure armour for tension-only case

| | **ITCODE31** | **ITCODE0** | **FULL FE** | **ANALYTICAL** |
|---|---|---|---|---|
| 6inch | -65 | -65 | -246 | -188 |
| 8inch | -56 | -56 | -90 | -102 |
| 16inch | -64 | -64 | -90 | -89 |

**Table 5.1.1:** Peak value of stress in carcass for tension-only case Unit: MPa

| | **ITCODE31** | **ITCODE0** | **FULL FE** | **ANALYTICAL** |
|---|---|---|---|---|
| 6inch | -348 | -348 | -195 | -188 |
| 8inch | -99 | -99 | -76 | -102 |
| 16inch | -91 | -91 | -78 | -89 |

**Table 5.1.2:** Peak value of stress in pressure armour for tension-only case Unit: MPa

According to the result, for ITCODE31 and ITCODE0, the stresses are exactly same both for carcass and pressure armour. This is because that the axisymmetric models

used in BFLEX for ITCODE31 and ITCODE0 are the same and the formulations used to compute the stress are same for subjecting a axial load. As expected, the stress in pressure armour is larger than that in carcass because that the plastic layer between carcass and pressure armour resist some of the stress. For full FE model, it shows that stress in carcass is smaller than that in pressure armour. The main reason is expected as that carcass, pressure armour and plastic layer between them are merged together. Therefore these three layers behave as a whole. And the axial stress is inversely proportional to the radius of layer. Hence, it appears that stress in carcass is larger, However, it is noted that the sum of stresses of full FE model is larger than that in other two models, which means that the plastic layer between carcass and pressure armour, named seal layer also, take less contact pressure in full FE model. This might due to more dofs are added in element HSHEAR363, making it softer. On analytical solution, the solution is a rough estimation based on the assumption that carcass and pressure armour merged together. Thus, the analytical stresses in carcass and pressure armour are same.

### 5.1.2 Axial stress in helical tensile layers

The axial stress in helical tensile layers for 6inch flexible pipe is represented in the following figure:

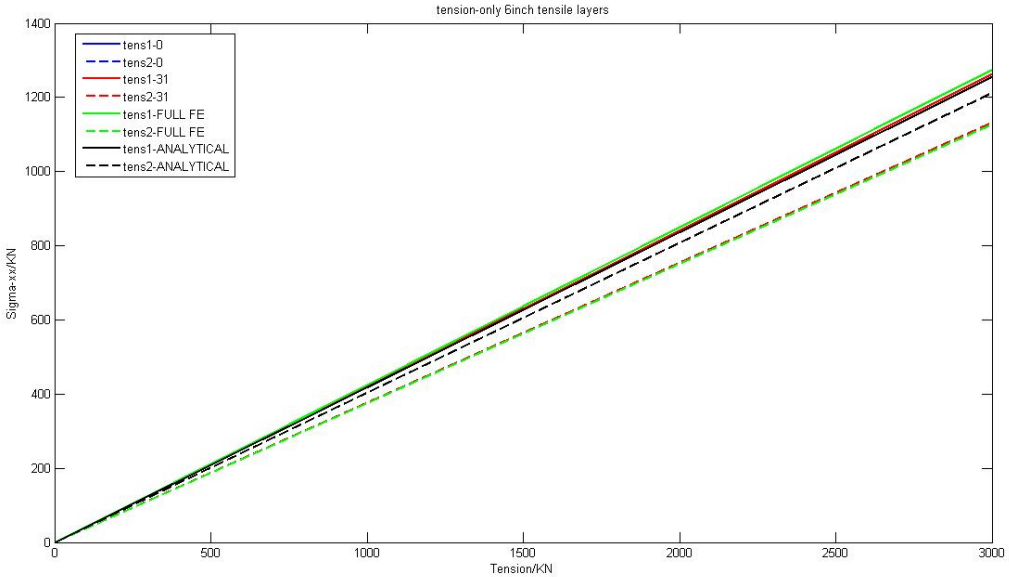


**Figure 5.5:** 6inch flexible stress distribution in helical tensile layers for tension-only case

The axial stress in helical tensile layers for 8inch flexible pipe:

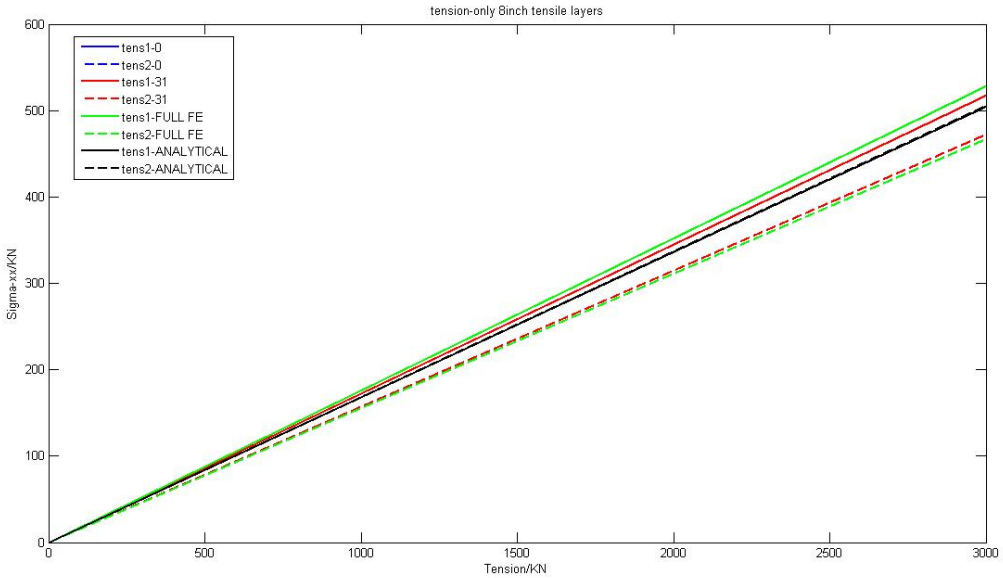


**Figure 5.6:** 8inch flexible stress distribution in helical tensile layers for tension-only case

The axial stress in helical tensile layers for 16inch flexible pipe:

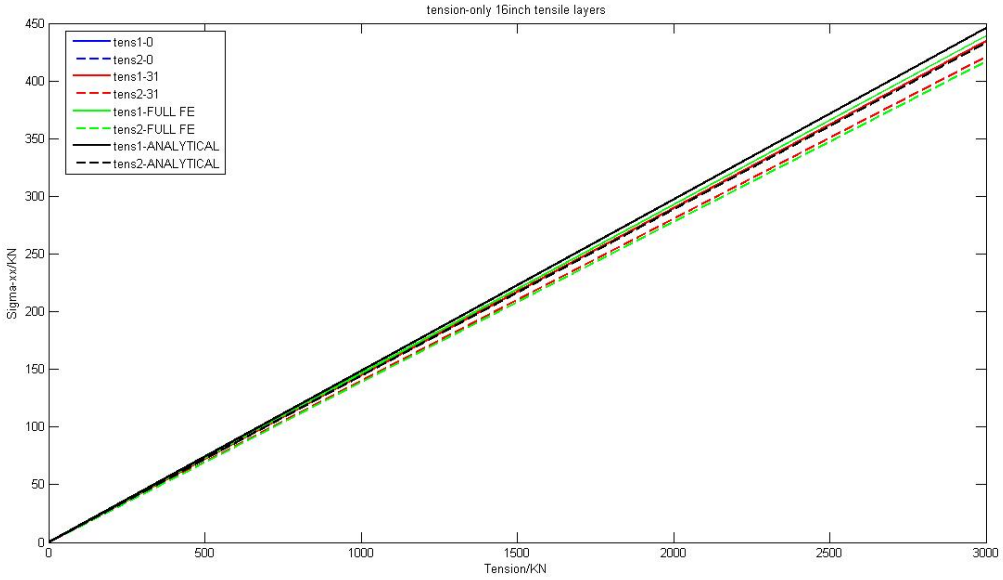


**Figure 5.7:** 16inch flexible stress distribution in helical tensile layers for tension-only case

Merge figures and extract the peak values:

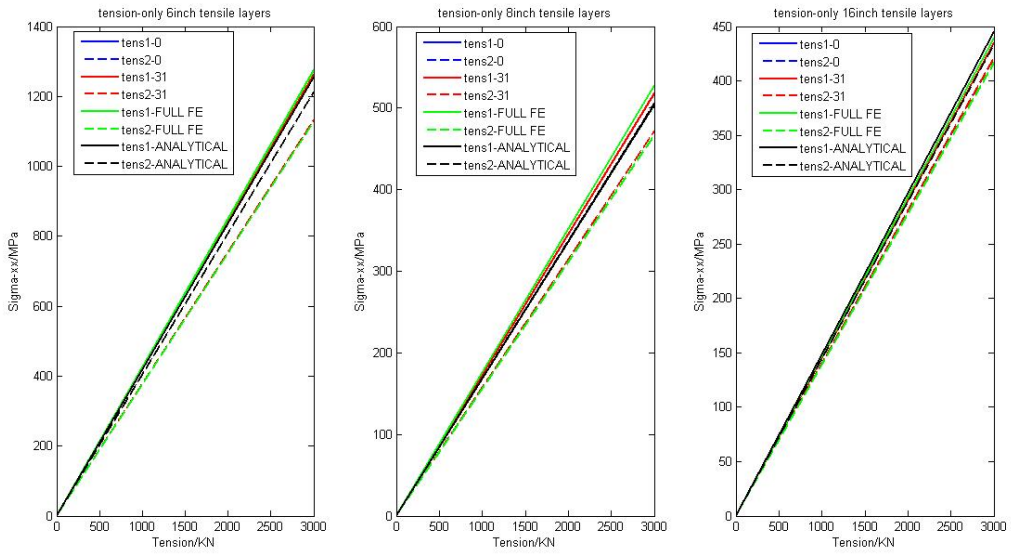


**Figure 5.8:** Stress distribution in helical tensile layers for tension-only case

| | ITCODE31 | ITCODE0 | FULL FE | ANALYTICAL |
|---|---|---|---|---|
| 6inch | 1262 | 1261 | 1275 | 1255 |
| 8inch | 518 | 518 | 528 | 504 |
| 16inch | 435 | 435 | 439 | 446 |

**Table 5.1.3:** Peak value of stress in 1st helical tensile layer for tension-only case Unit: MPa

| | ITCODE31 | ITCODE0 | FULL FE | ANALYTICAL |
|---|---|---|---|---|
| 6inch | 1132 | 1132 | 1127 | 1212 |
| 8inch | 472 | 472 | 467 | 506 |
| 16inch | 421 | 421 | 417 | 433 |

**Table 5.1.4:** Peak value of stress in 2nd helical tensile layer for tension-only case Unit: MPa

The result shows that the computing stresses fit the analytical solution well for all three models. Results from ITCODE31 and ITCODE0 are still same. Compared to the stresses in carcass and pressure armour, the stressed in helical tensile layers are lager, which means that most of the created stress is resisted by helical tensile layers as expected. Element

HSHEAR 353 contains more dof than other two elements. However, more dofs added into modelling element does not affect the result.

## 5.2 Internal pressure-only case

### 5.2.1 Axial stress in carcass and pressure Armour

The axial stress in carcass and pressure armour for 6inch flexible pipe is illustrated below:

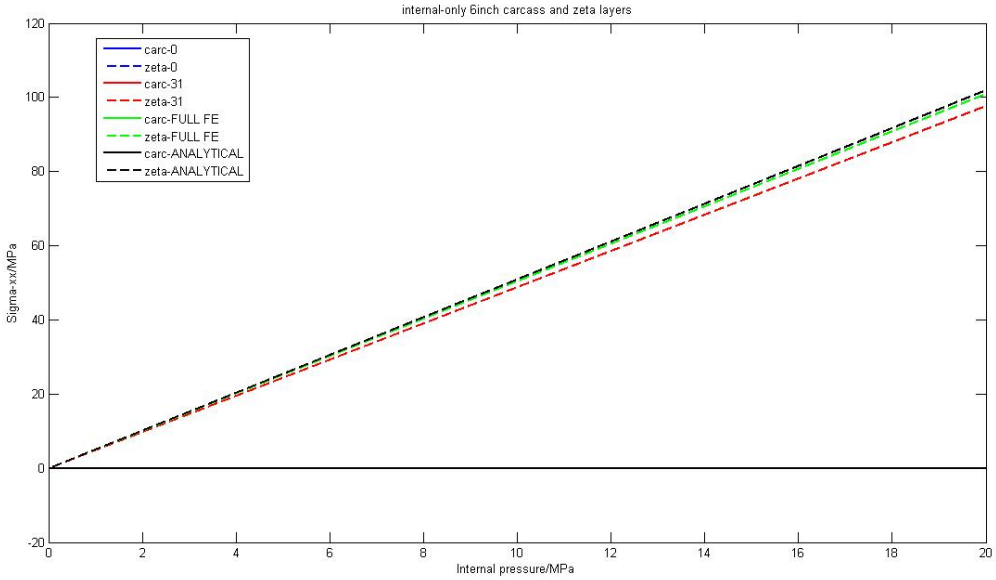


**Figure 5.9:** 6inch flexible pipe stress distribution in carcass and pressure armour for internal pressure-only case

The axial stress in carcass and pressure armour for 8inch flexible pipe is illustrated below:

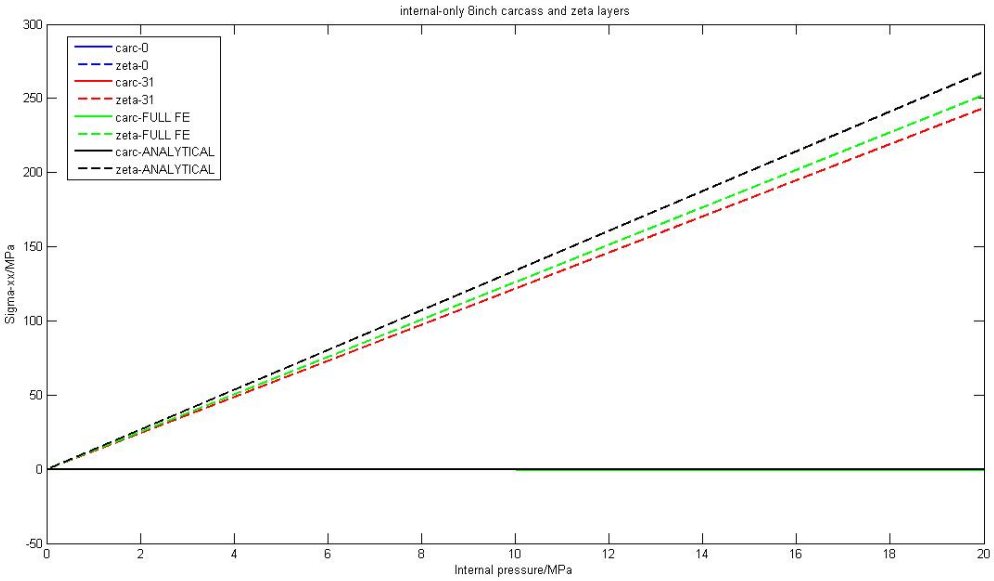


**Figure 5.10:** 8inch flexible pipe stress distribution in carcass and pressure armour for internal pressure-only case

The axial stress in carcass and pressure armour for 8inch flexible pipe is illustrated below:

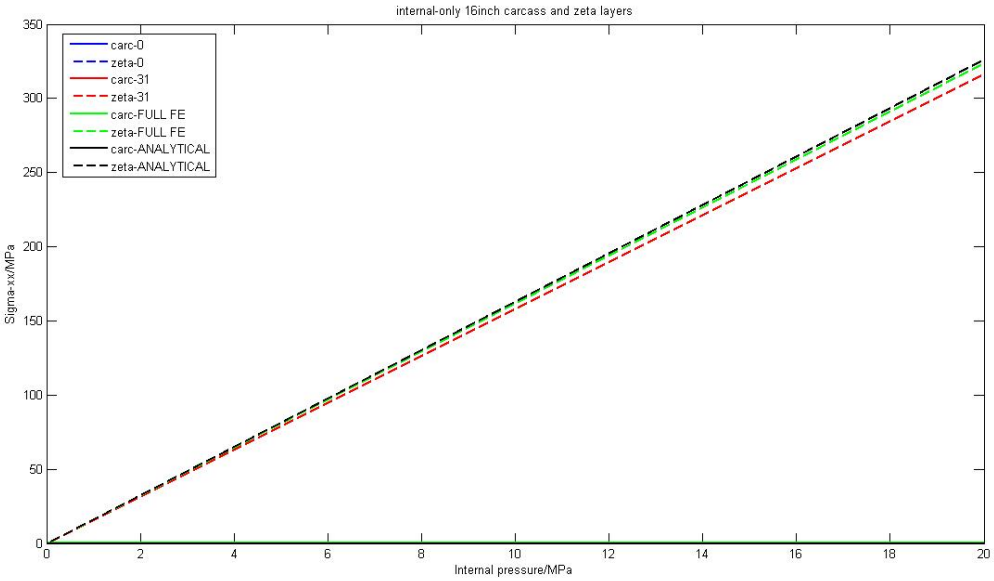


**Figure 5.11:** 16inch flexible pipe stress distribution in carcass and pressure armour for internal pressure-only case

For comparison, merge three figures into one and extract the peak values for each model and analytical solution:

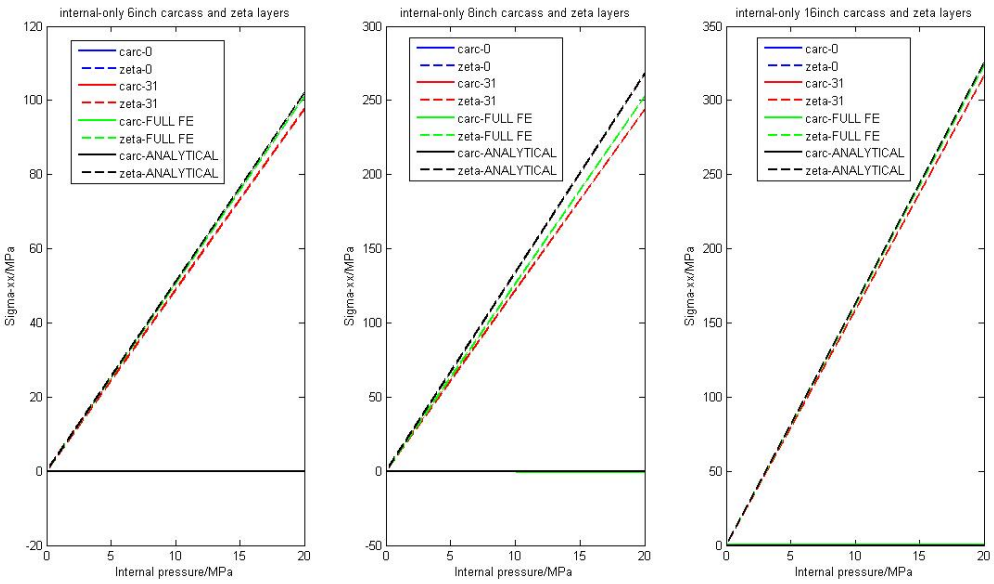


**Figure 5.12:** Stress distribution in carcass and pressure armour for internal pressure-only case

| | ITCODE31 | ITCODE0 | FULL FE | ANALYTICAL |
|---|---|---|---|---|
| 6inch | 0 | 0 | -0.07 | 0 |
| 8inch | 0.05 | -0.5 | -90 | 0 |
| 16inch | 0 | 0 | 0.1 | 0 |

**Table 5.2.1:** Peak value of stress in carcass for internal pressure-only case Unit: MPa

| | ITCODE31 | ITCODE0 | FULL FE | ANALYTICAL |
|---|---|---|---|---|
| 6inch | 98 | 98 | 101 | 61 |
| 8inch | 244 | 244 | 253 | 83 |
| 16inch | 316 | 316 | 323 | 158 |

**Table 5.2.2:** Peak value of stress in pressure armour for internal pressure-only case Unit: MPa

Result shows that carcass almost doesn't take any axial stress as expected. For pressure armour, computing values fit the analytical values well. For ITCODE31 and ITCODE0 model, the computing results are still same. For the load case, in full FE model, carcass,

pressure and seal layer between them are merged as well and carcass is fixed so that the pressure acts on pressure armour and is resisted partly by seal layer. As mentioned above, more dofs are introduced in element HSHEAR363 and make it softer. Thus it might absorb less created stress. Therefore, similarly, it appears that larger stress is in full FE model.

### 5.2.2 Axial stress in helical tensile layers

The axial stress in helical tensile layers for 6inch flexible pipe is represented in the following figure:

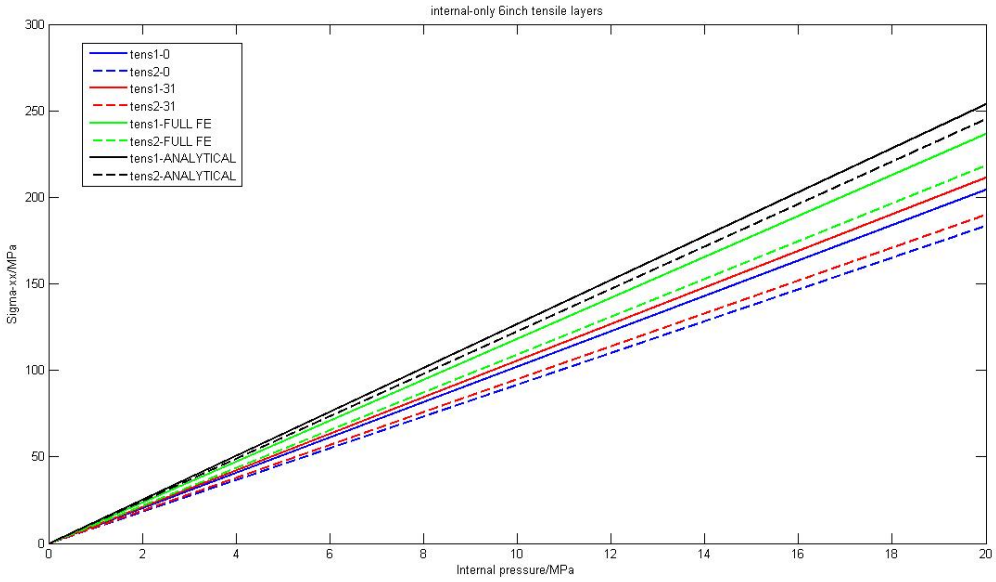


**Figure 5.13:** 6inch flexible stress distribution in helical tensile layers for internal pressure-only case

The axial stress in helical tensile layers for 8inch flexible pipe:

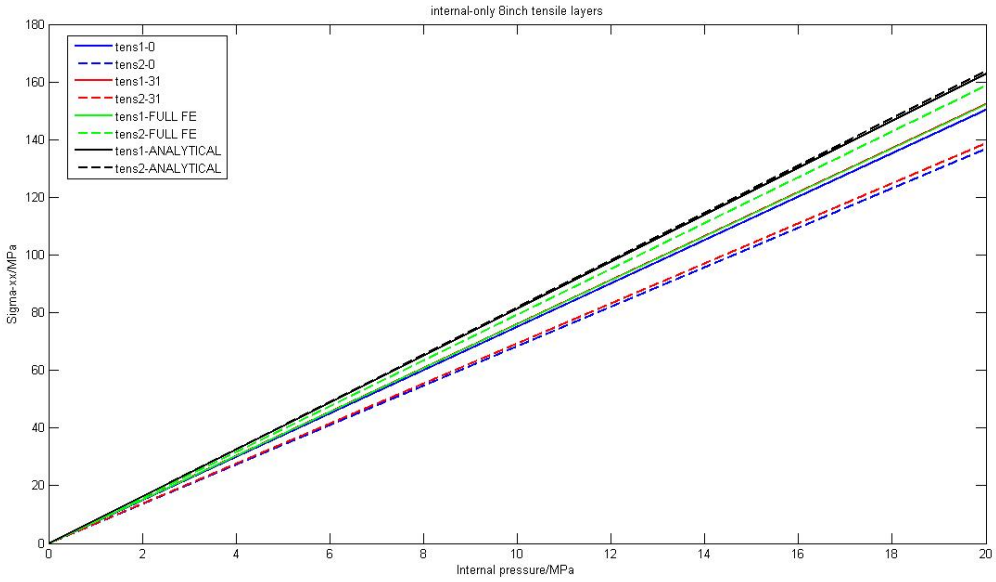


**Figure 5.14:** 8inch flexible stress distribution in helical tensile layers for internal pressure-only case

The axial stress in helical tensile layers for 16inch flexible pipe:

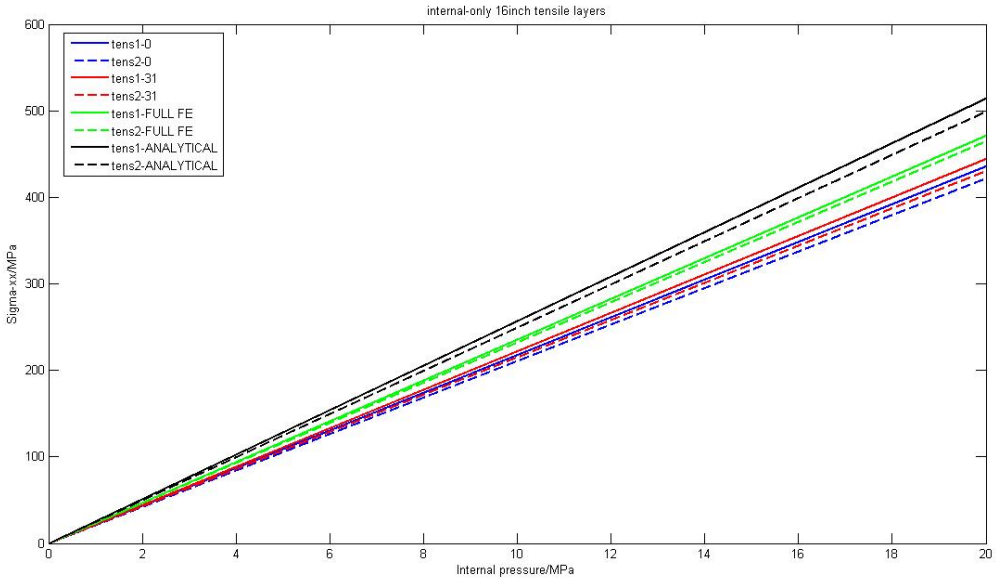


**Figure 5.15:** 16inch flexible stress distribution in helical tensile layers for internal pressure-only case

Merge figures and extract the peak values:

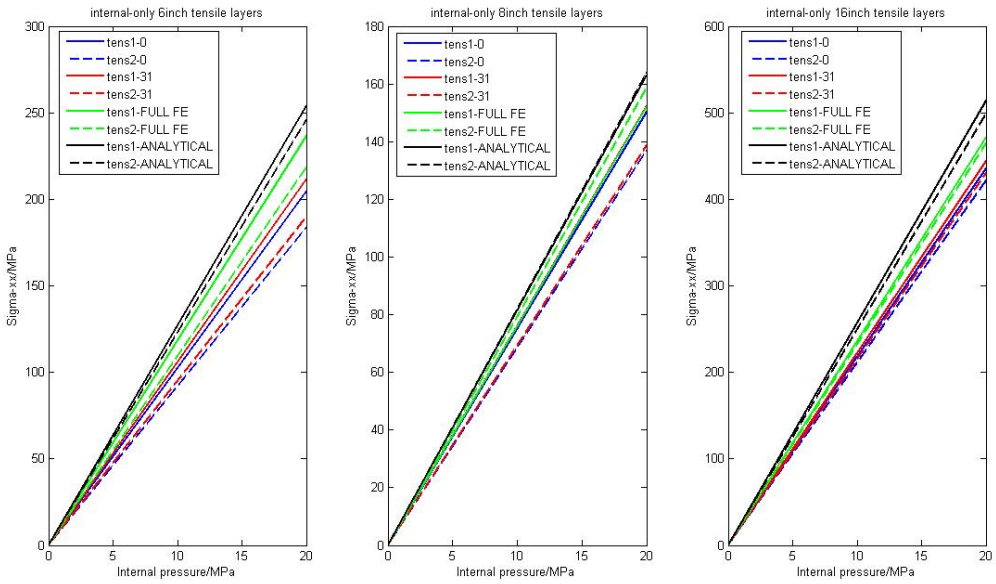


**Figure 5.16:** Stress distribution in helical tensile layers for internal pressure-only case

| | ITCODE31 | ITCODE0 | FULL FE | ANALYTICAL |
|---|---|---|---|---|
| 6inch | 211 | 205 | 236 | 254 |
| 8inch | 152 | 150 | 152 | 163 |
| 16inch | 444 | 436 | 472 | 514 |

**Table 5.2.3:** Peak value of stress in 1st helical tensile layer for internal pressure-only case Unit: MPa

| | ITCODE31 | ITCODE0 | FULL FE | ANALYTICAL |
|---|---|---|---|---|
| 6inch | 190 | 184 | 219 | 245 |
| 8inch | 139 | 137 | 159 | 164 |
| 16inch | 430 | 422 | 465 | 499 |

**Table 5.2.4:** Peak value of stress in 2nd helical tensile layer for internal pressure-only case Unit: MPa

For the load case, in ITCODE31, all layers are modelled by element PIPE52. In ITCODE0 model, tensile layers are modelled by element HSHEAR352 while other layers are modelled

by element PIPE52. HSHEAR352 contains more dof than PIPE52, which might be the reason that lowest curves appear in ITCODE0 model for both two tensile layers. The curves of full FE are highest. It might be considered that softer element are used to model plastic layers. Analytical solution is assumed all created load acting on tensile layers, meaning that resistance of plastic layers is not considered. This might be the reason that all computing values are smaller than the analytical values.

## 5.3 External pressure-only case

### 5.3.1 Axial stress in carcass and pressure Armour

The axial stress in carcass and pressure armour for 6inch flexible pipe is illustrated below:

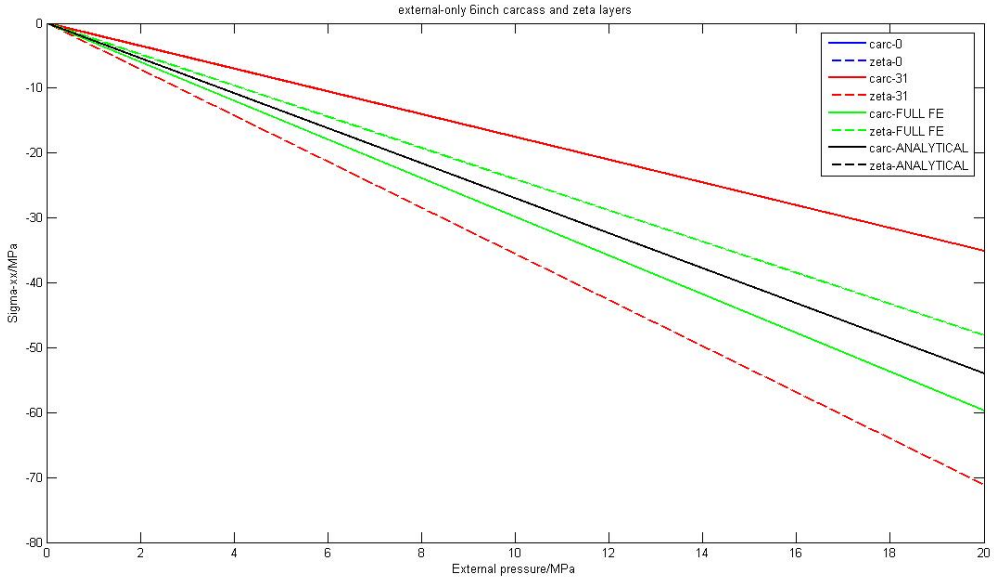


**Figure 5.17:** 6inch flexible pipe stress distribution in carcass and pressure armour for external pressure-only case

The axial stress in carcass and pressure armour for 8inch flexible pipe is illustrated below:

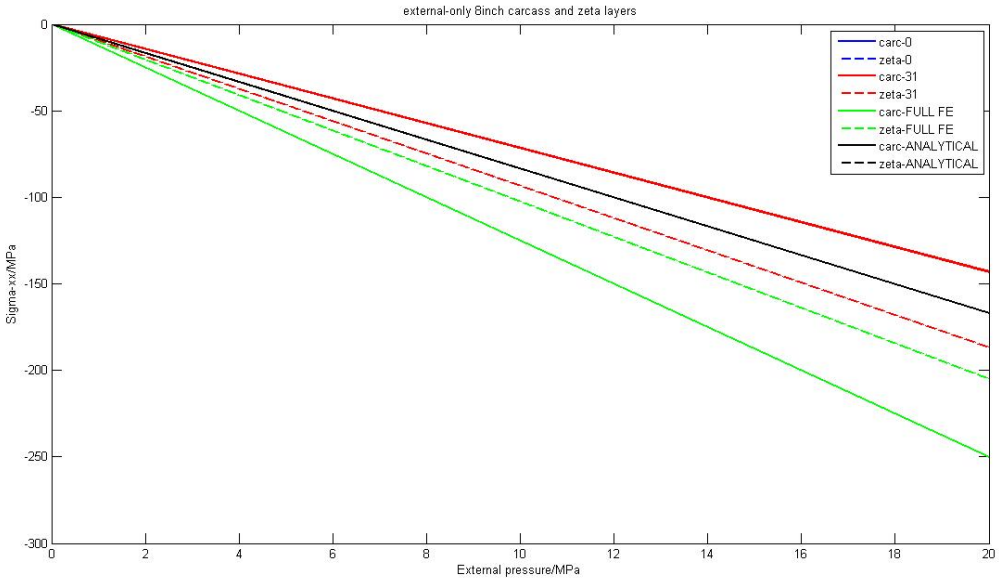


**Figure 5.18:** 8inch flexible pipe stress distribution in carcass and pressure armour for external pressure-only case

The axial stress in carcass and pressure armour for 8inch flexible pipe is illustrated below:

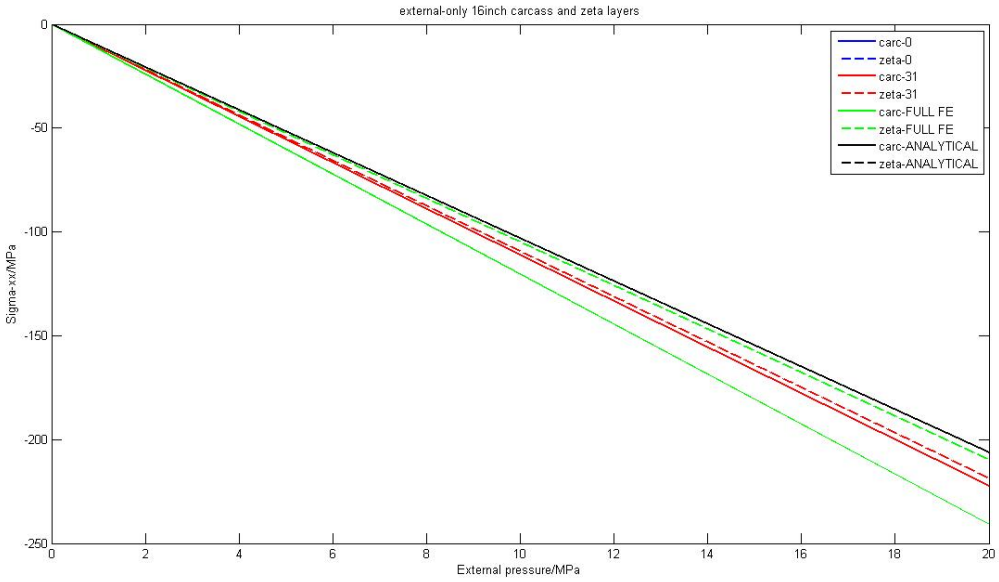


**Figure 5.19:** 16inch flexible pipe stress distribution in carcass and pressure armour for external pressure-only case

For comparison, merge three figures into one and extract the peak values for each model and analytical solution:

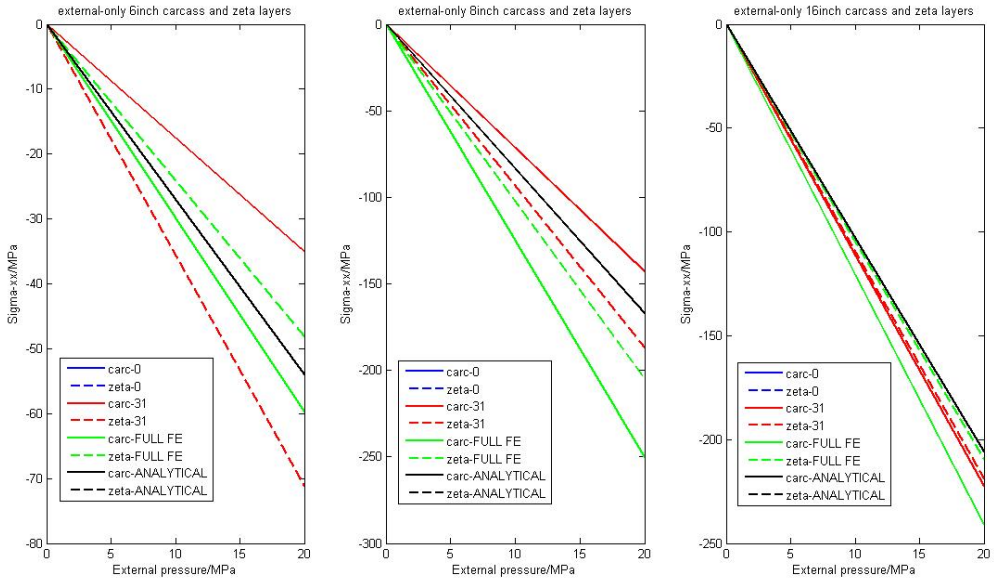


**Figure 5.20:** Stress distribution in carcass and pressure armour for external pressure-only case

| | ITCODE31 | ITCODE0 | FULL FE | ANALYTICAL |
|---|---|---|---|---|
| 6inch | -35 | -35 | -60 | -54 |
| 8inch | -143 | -143 | -251 | -167 |
| 16inch | -222 | -222 | -248 | -207 |

**Table 5.3.1:** Peak value of stress in carcass for external pressure-only case Unit: MPa

| | ITCODE31 | ITCODE0 | FULL FE | ANALYTICAL |
|---|---|---|---|---|
| 6inch | -71 | -71 | -48 | -54 |
| 8inch | -187 | -187 | -205 | -167 |
| 16inch | -219 | -219 | -216 | -206 |

**Table 5.3.2:** Peak value of stress in pressure armour for external pressure-only case Unit: MPa

From results, since the introduced external pressure is acting on the outersheath, expectedly, for ITCODE31 and ITCODE0 models, the axial stress in pressure armour is larger compared to the stress in carcass. Because the created load is resisted by metallic layers

in the order from outside to inside. For full FE model, carcass and pressure armour is merged to one same coordinate system, so they behave together when modelling, which is also the reason that the large axial stress occurs in carcass. The analytical solutions are same for carcass and pressure armour because they are assumed to be one layer when calculating. For three models, it is noted that the sum of the stresses in carcass and pressure almost equal to the sum of both two analytical solution. However, in 8inch pipe, results are not very good. This might due to that there is a thick layer outersheath surrounding the pipe.

### 5.3.2 Axial stress in helical tensile layers

The axial stress in helical tensile layers for 6inch flexible pipe is represented in the following figure:

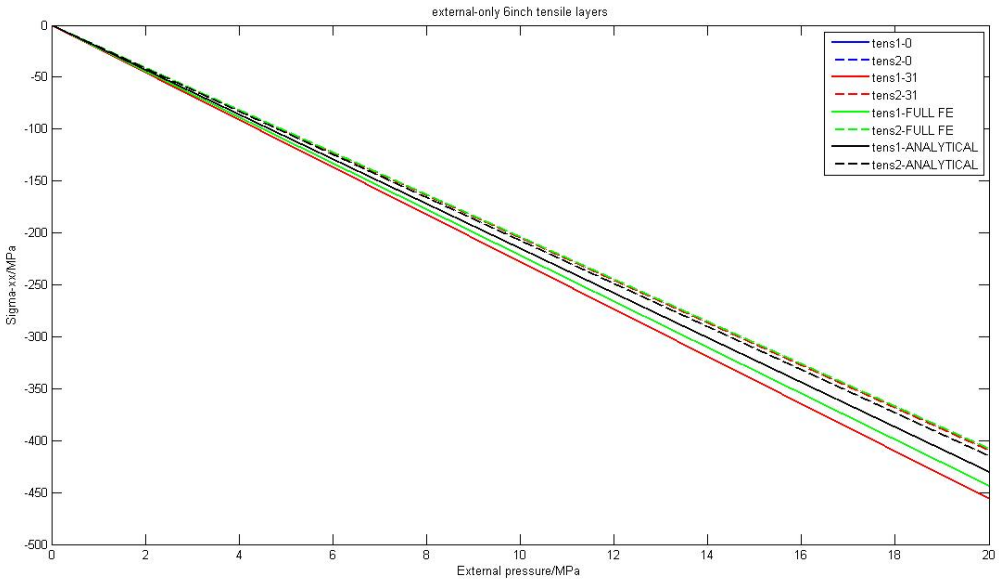


**Figure 5.21:** 6inch flexible stress distribution in helical tensile layers for external pressure-only case

The axial stress in helical tensile layers for 8inch flexible pipe:

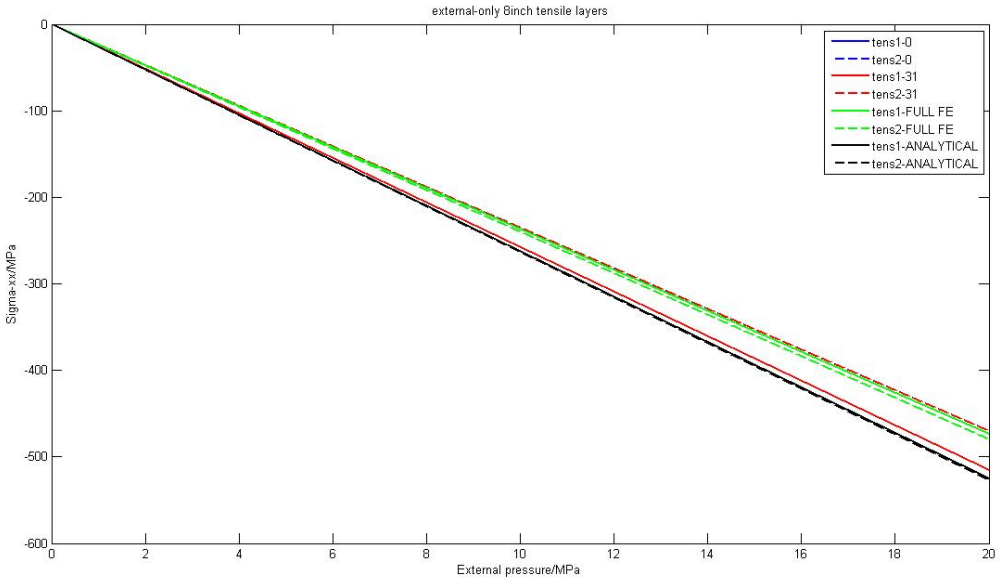


**Figure 5.22:** 8inch flexible stress distribution in helical tensile layers for external pressure-only case

The axial stress in helical tensile layers for 16inch flexible pipe:

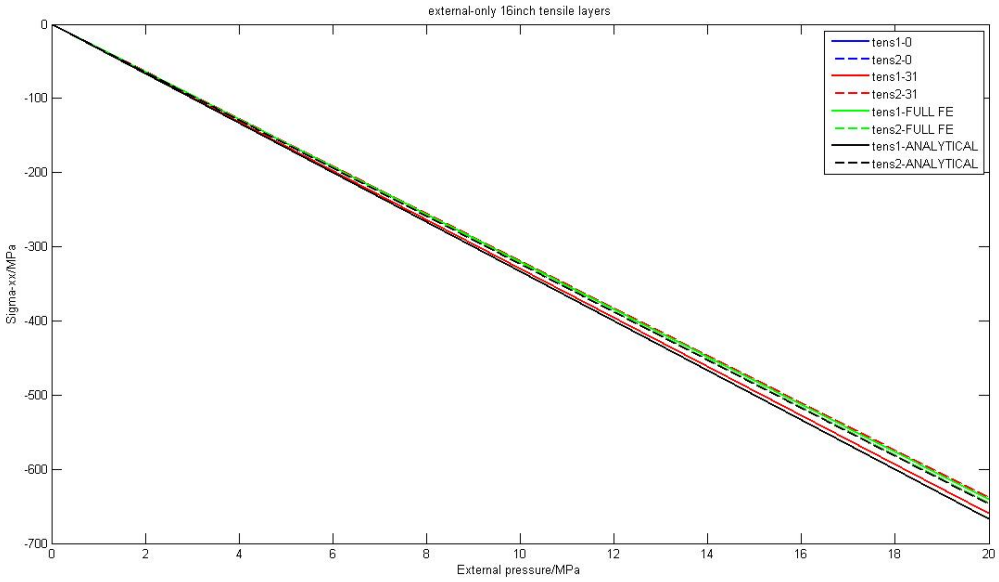


**Figure 5.23:** 16inch flexible stress distribution in helical tensile layers for external pressure-only case

Merge figures and extract the peak values:

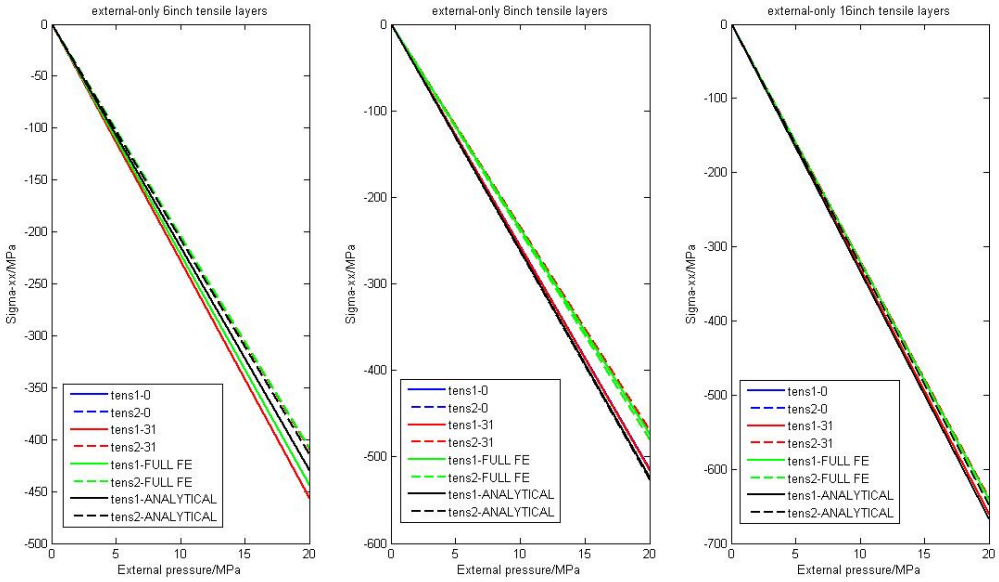


**Figure 5.24:** Stress distribution in helical tensile layers for external pressure-only case

| | ITCODE31 | ITCODE0 | FULL FE | ANALYTICAL |
|---|---|---|---|---|
| 6inch | -456 | -456 | -444 | -430 |
| 8inch | -515 | -515 | -474 | -525 |
| 16inch | -660 | -660 | -641 | -667 |

**Table 5.3.3:** Peak value of stress in 1st helical tensile layer for external pressure-only case Unit: MPa

| | ITCODE31 | ITCODE0 | FULL FE | ANALYTICAL |
|---|---|---|---|---|
| 6inch | -409 | -409 | -408 | -416 |
| 8inch | -470 | -470 | -480 | -527 |
| 16inch | -639 | -639 | -646 | -648 |

**Table 5.3.4:** Peak value of stress in 2nd helical tensile layer for external pressure-only case Unit: MPa

Results show that most of the computing values fit the analytical solutions. As expected, for ITCODE31 and ITCODE0, the axial stress in pressure armour is larger compared to

that in carcass. For full FE model, since the carcass and pressure armour are merged to one coordinate system and behave together, a converse trend occurs.

# Chapter 6

# Conclusion

## 6.1 Concluding remarks

BFLEX program can be used to model flexible pipe subjected axisymmetric load and compute the axial stress in metallic layers. For ITCODE31 and ITCODE0 models, the computing stresses are reasonable and almost same from element PIPE52 and HSHEAR352. The stresses are normally smaller than the stress from element HSHEAR353. For full FE model, performance of element HSHEAR353 on modelling helical tensile layer is acceptable. The computing stresses from element HSHEAR353 can be concluded fitting the analytical solutions. There is almost no large deviation between the computing stresses and analytical solutions. Therefore, on modeling helical tensile layer subjected axisymmetric load, results are acceptable for all three elements. On the other hand, for ITCODE31 and ITCODE0, by using element PIPE52, performance of modelling carcass and pressure armour is acceptable, showing a reasonable stress distribution in those two metallic layers and a good-fitting sum of stress. For full FE, the result is less satisfied except for the load case of internal pressure acting only. Mergence of carcass and pressure armour replaces defining a contact layer between them, which consequent a less satisfied results. Moreover, added dof makes element softer. However, this does not bring large effects to axial stress in metallic layers when axisymmetric load acting.

## 6.2 Suggestion to future work

During modelling, for full FE model, to model the pipe subjected tension only and external pressure only, one need to do is merging carcass, pressure armour and seal layers between them into one coordinate system. This is because that currently there is no a direct way to define the contact layer between carcass and pressure armour. Because the HSHEAR363 element is defined in cartesian coordinate system while contact elements are used to connect elements defined in polar coordinate system. The current contact elements, i.e. HCONT453 and HCONT463, are 4 noded element. They can not be used to establish connection between two HSHEAR363 elements. The consequence of the mergence is that stress in carcass is larger than in pressure armour, which is converse to the actual situation. This is also the case in internal-only case. Merely, for internal pressure-only case, the carcass layer is fixed due to that it does take any stress expectedly. Therefore, an improvement to coordinate system or new contact element which are used to connect two HSHEAR363 elements might be the point of the future work.

# Bibliography


[1] S. Sævik. *Lecture Notes in Offshore Pipeline Technology*, 02 2013.

[2] S. Sævik. *On Stresses and Fatigue in Flexible Pipes*. PhD thesis, NTH, Trondheim, Norway, 1992.

[3] Bournazel C. Feret, J. and J. Rigaud. Evaluation of flexible pipes life expectancy under dynamic conditions. In *OTC5230, Houston, USA*. Offshore Technology Conference, 1986.

[4] S. Sævik. A finite element model for predicting stresses and slip in flexible pipe armouring tendons. *Computers and Structures*, 46(2):219 – 230, 1993.

[5] S. Sævik, O. D. Økland, G. S. Baarholm, and J. Gjøsteen. Bflex2010 - *Users Manual*. MARINTEK, Trondheim, Norway, 2009. Marintek Document.

[6] S. Sævik. Bflex2010 - *Theory Manual*. MARINTEK, Trondheim, Norway, 2010.

[7] A. Custodio and M. Vaz. A nonlinear formulation for the axisymmetric response of umbilical cables and flexible pipes. In *J. of Applied Ocean Research ,24*, pages 21–29, 2002.

[8] Svein Sævik. Theoretical and experimental studies of stresses in flexible pipes. *Computers and Structures*, 89(23):2273 – 2291, 2011.

[9] J.A.Witz and Z.Tan. On the flexural structural behaviour of flexible pipes, umbilicals and marine cables. *Marine Structures*, 5:229 – 249, 1992.

[10] Engseth A. Fylling I. Larsen C.M. Leira B.J. Nygaard I. Berge, S. and A. Olufsen. *Handbook on Design and Operation of Flexible Pipes*. SINTEF, N-7034,Trondheim, Norway, 02 1992.

# Appendix A

# Models for 6inch flexible pipe

## A.1 Tension-only case

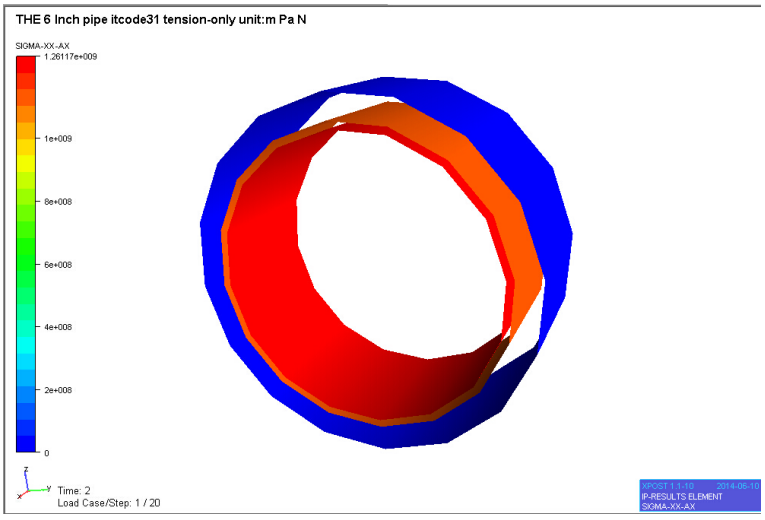


**Figure A.1:** 6inch flexible pipe model in BFLEX for ITCODE31

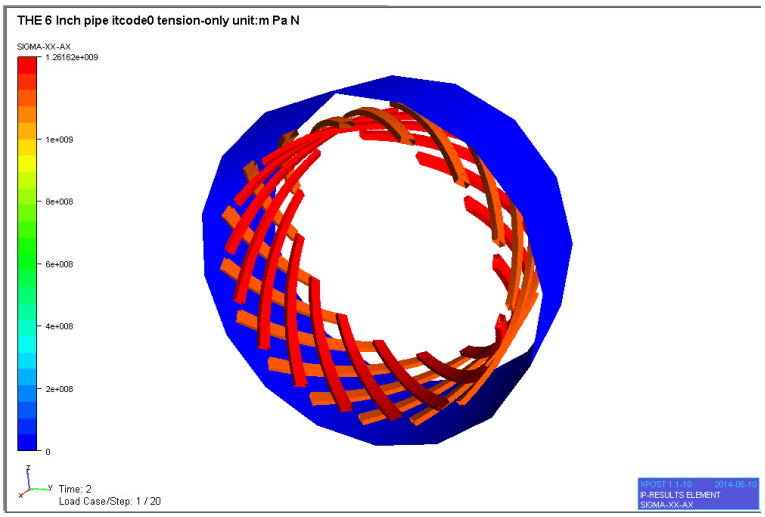


**Figure A.2:** 6inch flexible pipe model in BFLEX for ITCODE0

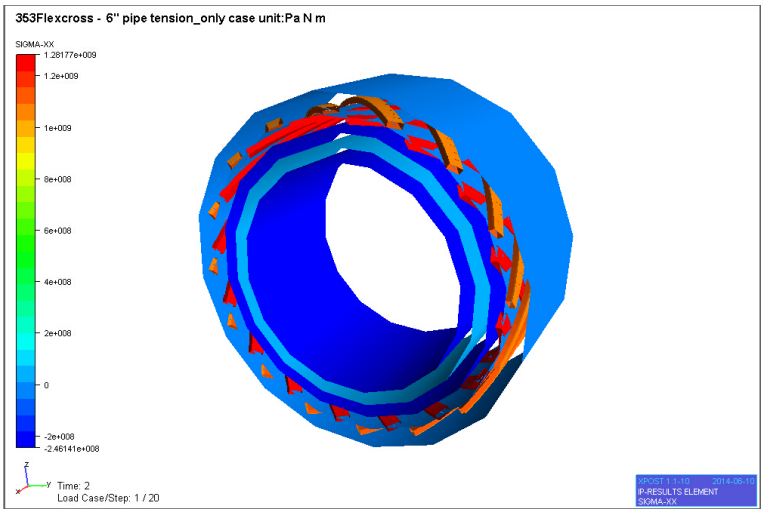


**Figure A.3:** 6inch flexible pipe model in BFLEX for full FE

## A.2 Internal pressure-only case

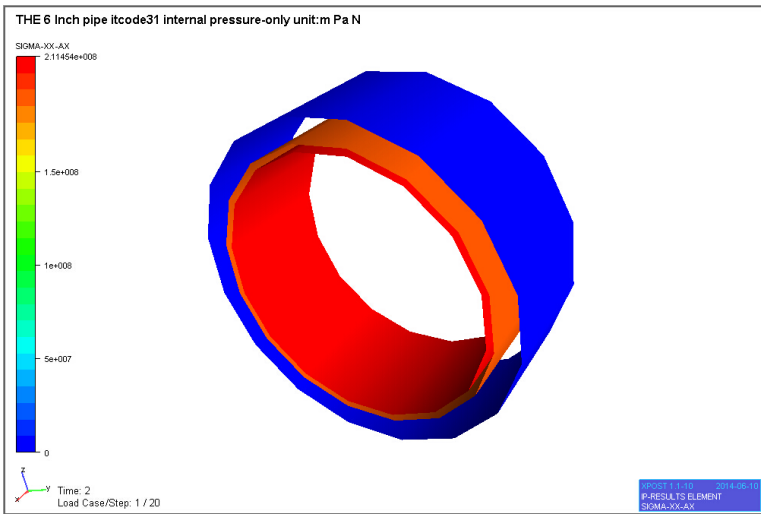


**Figure A.4:** 6inch flexible pipe model in BFLEX for ITCODE31

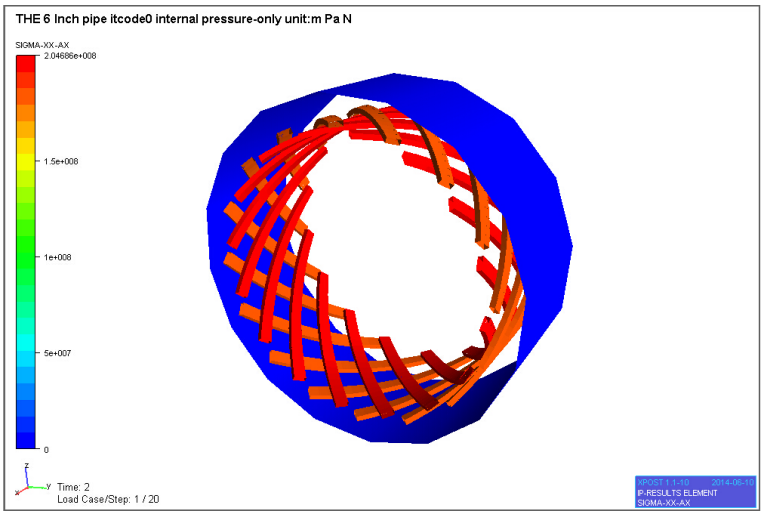


**Figure A.5:** 6inch flexible pipe model in BFLEX for ITCODE0

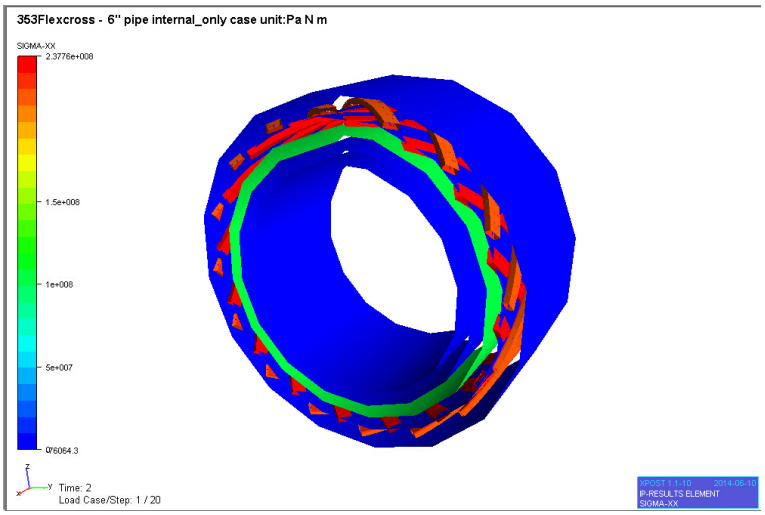


**Figure A.6:** 6inch flexible pipe model in BFLEX for full FE

## A.3 External pressure-only case

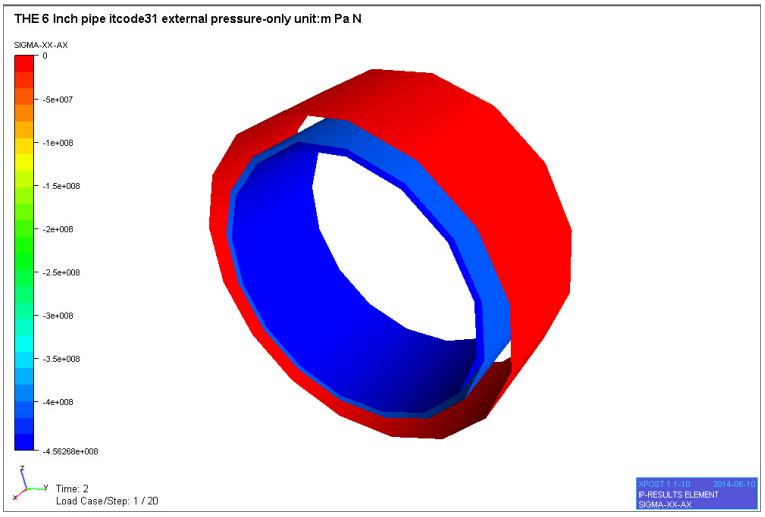


**Figure A.7:** 6inch flexible pipe model in BFLEX for ITCODE31

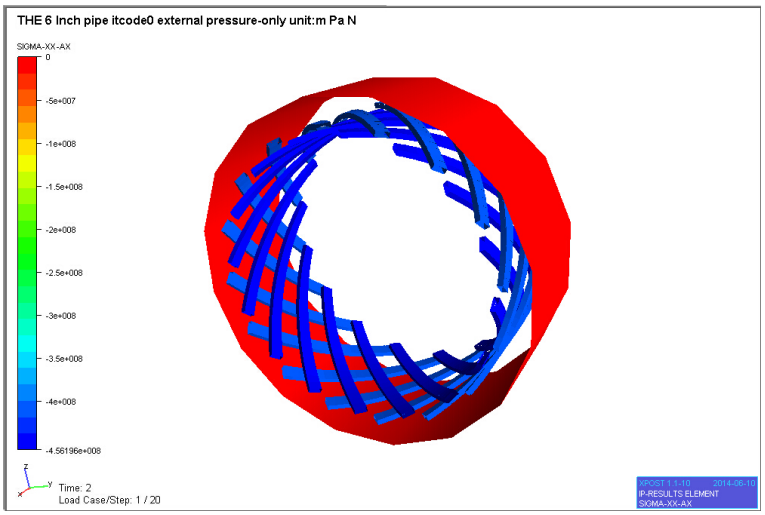


**Figure A.8:** 6inch flexible pipe model in BFLEX for ITCODE0

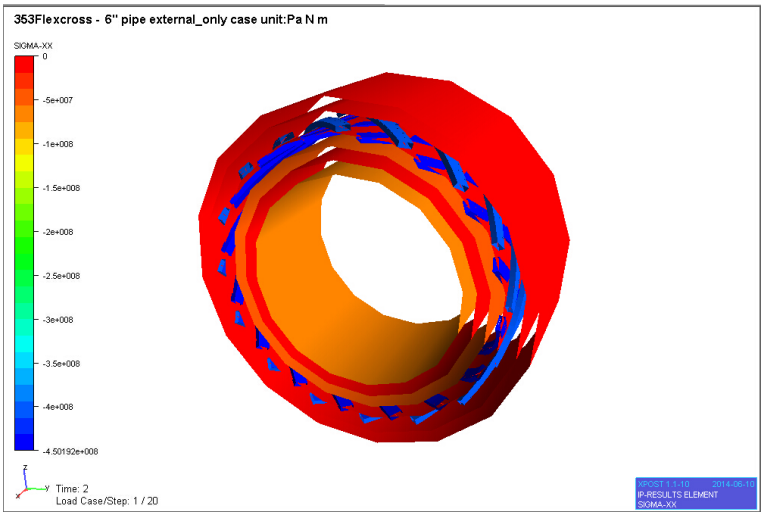


**Figure A.9:** 6inch flexible pipe model in BFLEX for full FE

# Appendix B

# Models for 8inch flexible pipe

## B.1 Tension-only case

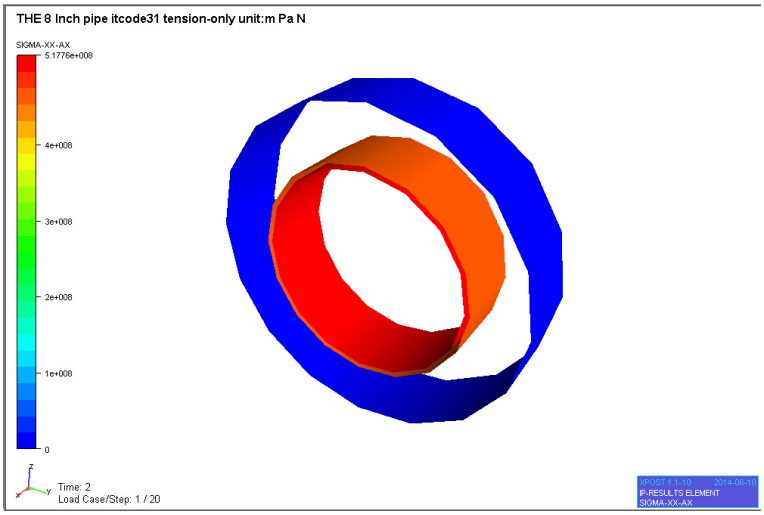


**Figure B.1:** 8inch flexible pipe model in BFLEX for ITCODE31

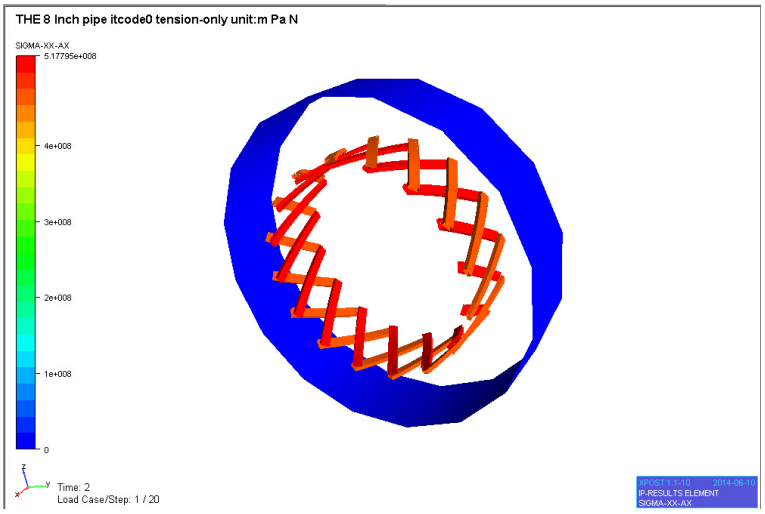


**Figure B.2:** 8inch flexible pipe model in BFLEX for ITCODE0

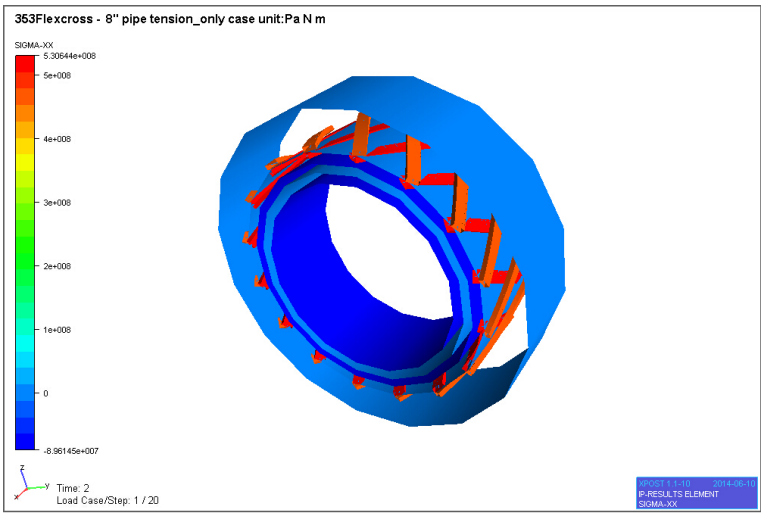


**Figure B.3:** 8inch flexible pipe model in BFLEX for full FE

## B.2 Internal pressure-only case

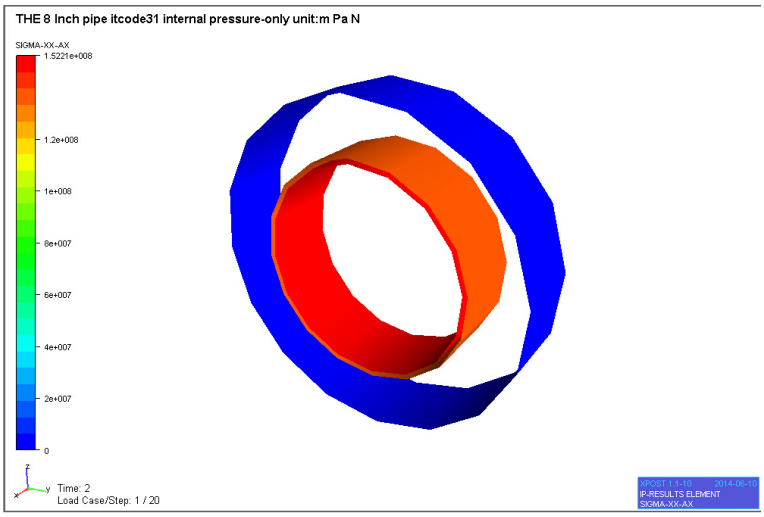


**Figure B.4:** 8inch flexible pipe model in BFLEX for ITCODE31

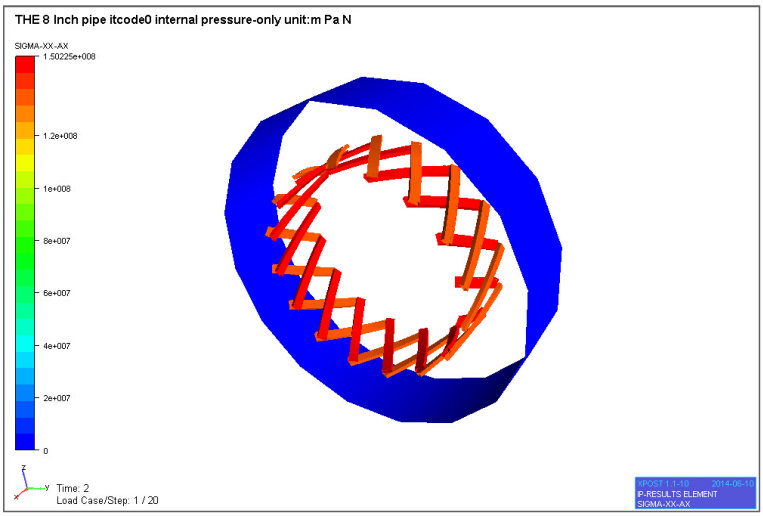


**Figure B.5:** 8inch flexible pipe model in BFLEX for ITCODE0

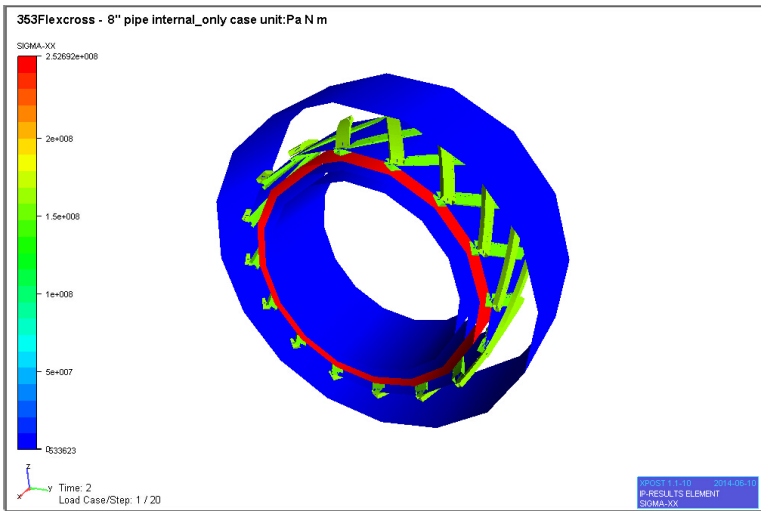


**Figure B.6:** 8inch flexible pipe model in BFLEX for full FE

## B.3 External pressure-only case

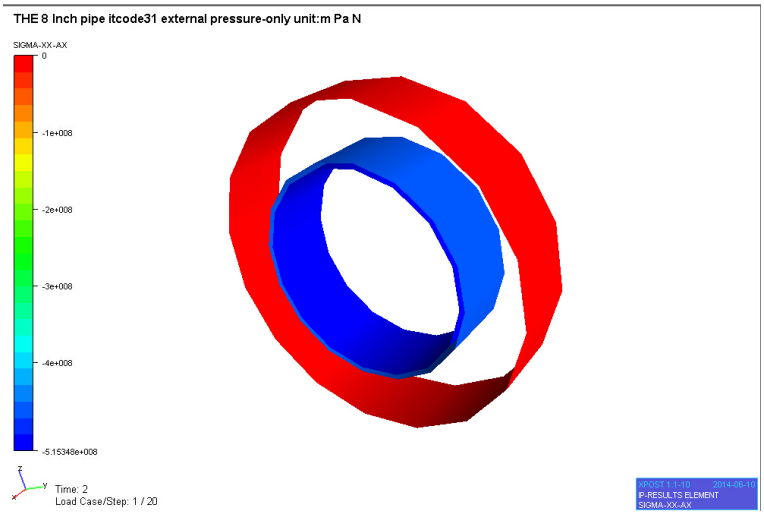


**Figure B.7:** 8inch flexible pipe model in BFLEX for ITCODE31

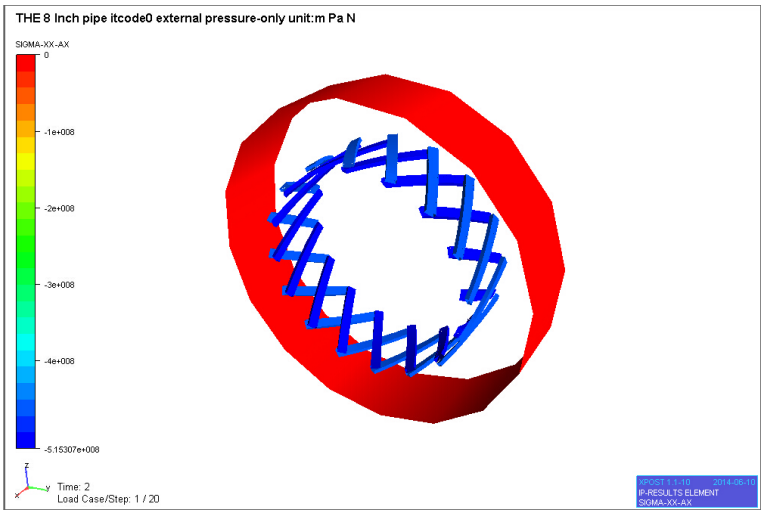


**Figure B.8:** 8inch flexible pipe model in BFLEX for ITCODE0

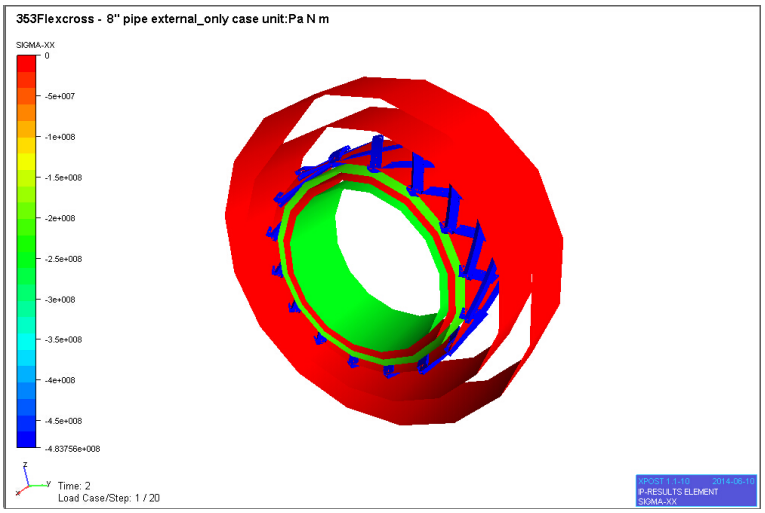


**Figure B.9:** 8inch flexible pipe model in BFLEX for full FE

# Appendix C

# Models for 16inch flexible pipe

## C.1 Tension-only case

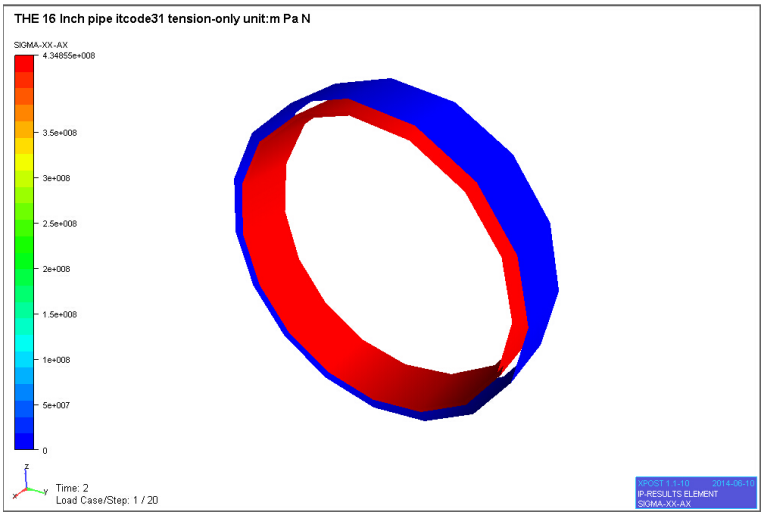


**Figure C.1:** 16inch flexible pipe model in BFLEX for ITCODE31

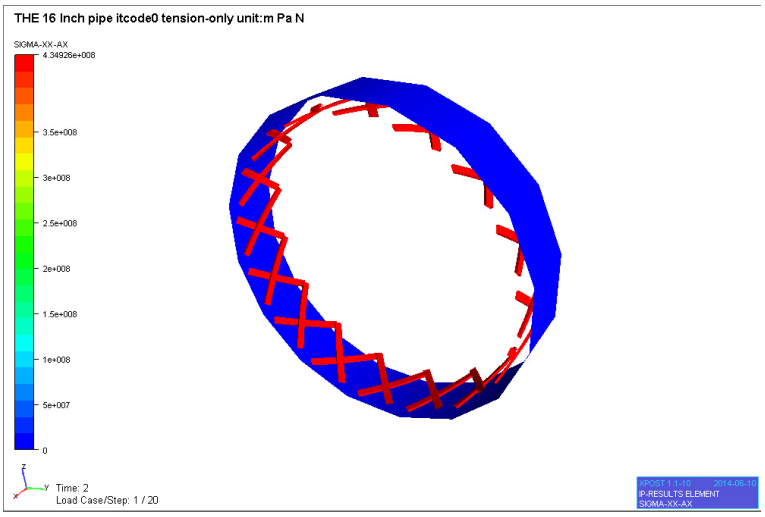


**Figure C.2:** 16inch flexible pipe model in BFLEX for ITCODE0

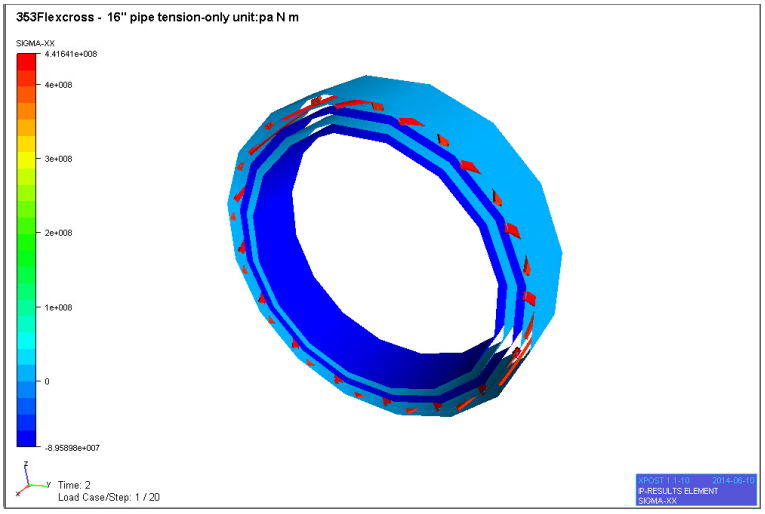


**Figure C.3:** 16inch flexible pipe model in BFLEX for full FE

## C.2 Internal pressure-only case

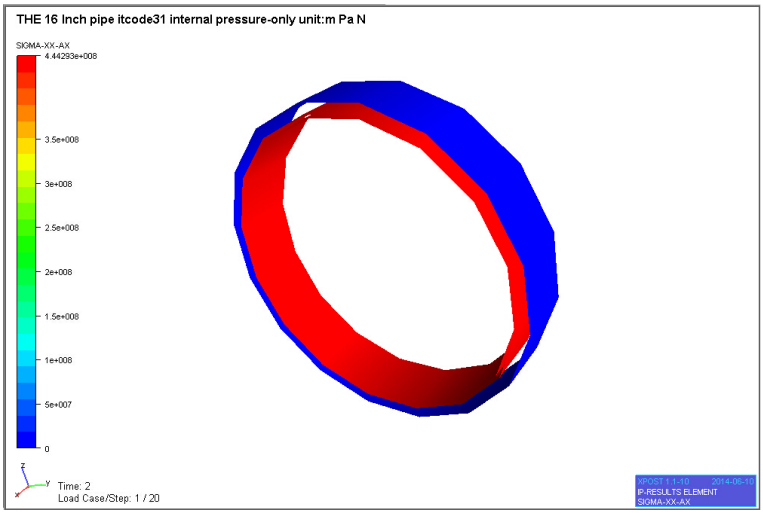


**Figure C.4:** 16inch flexible pipe model in BFLEX for ITCODE31

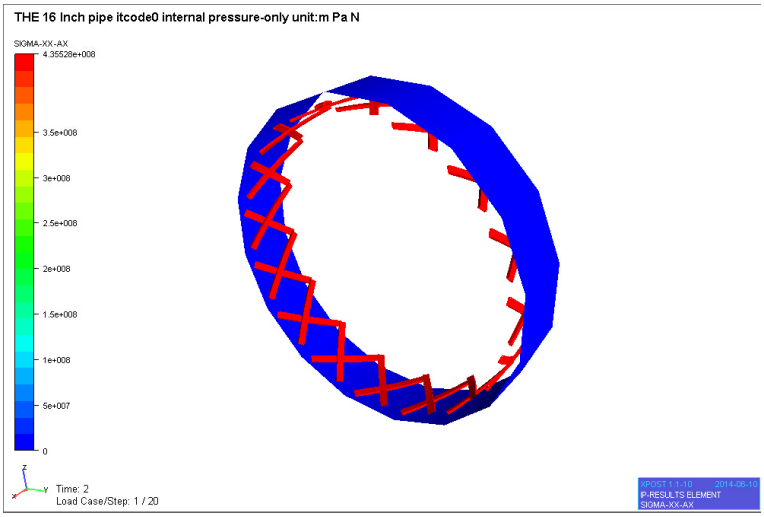


**Figure C.5:** 16inch flexible pipe model in BFLEX for ITCODE0

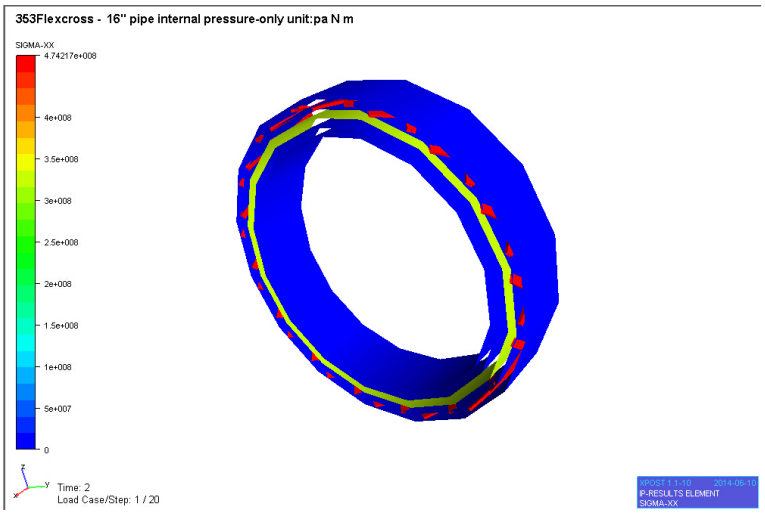


**Figure C.6:** 16inch flexible pipe model in BFLEX for full FE

## C.3 External pressure-only case

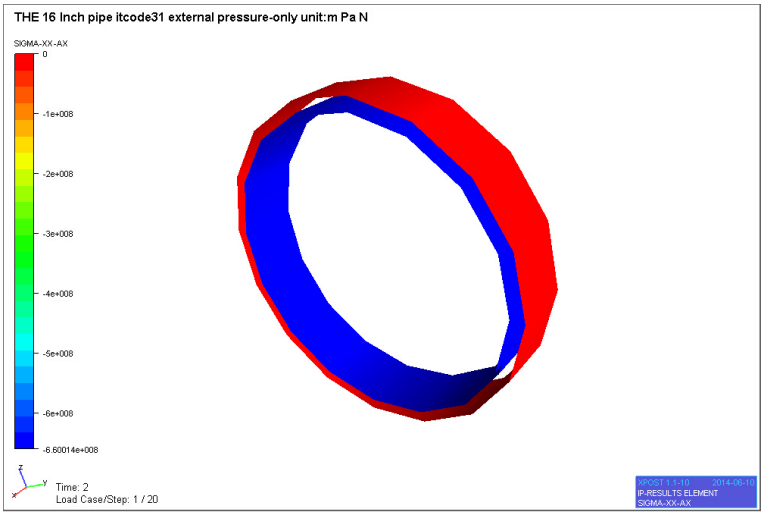


**Figure C.7:** 16inch flexible pipe model in BFLEX for ITCODE31

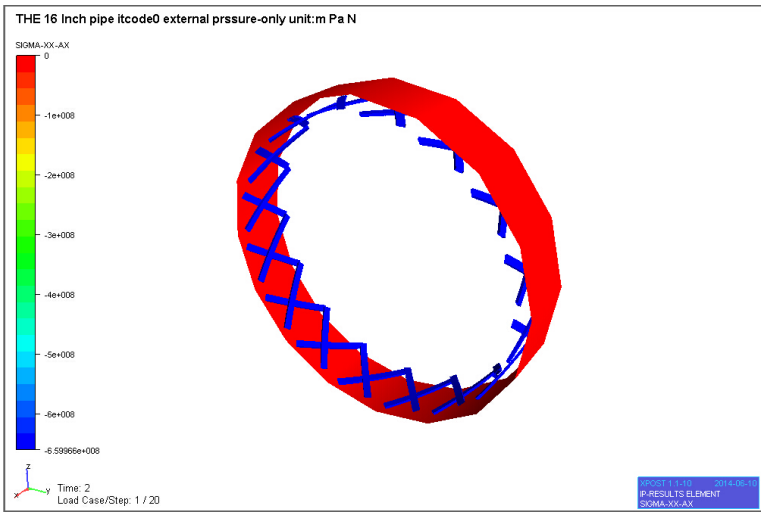


**Figure C.8:** 16inch flexible pipe model in BFLEX for ITCODE0

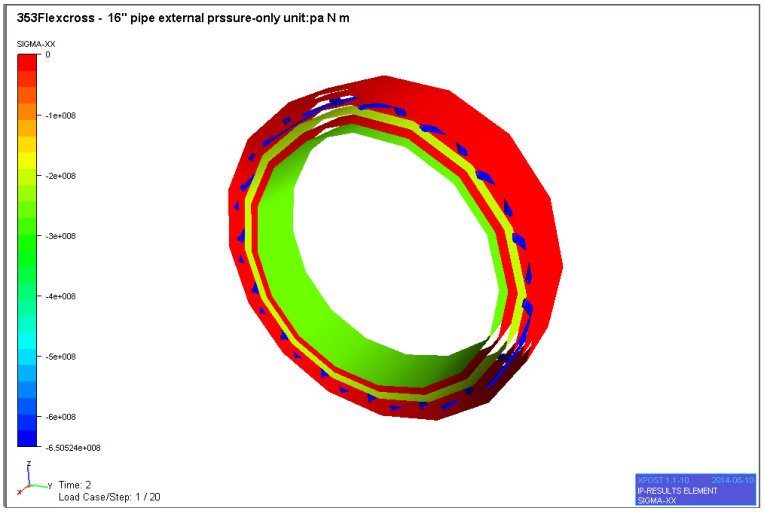


**Figure C.9:** 16inch flexible pipe model in BFLEX for full FE